

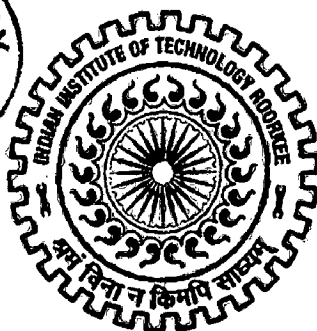
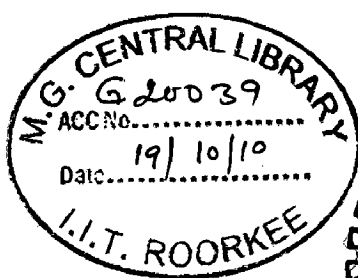
# **ADSORPTIVE DESULFURIZATION USING ACTIVATED CARBON**

**A DISSERTATION**

*Submitted in partial fulfillment of the  
requirements for the award of the degree  
of*  
**MASTER OF TECHNOLOGY**  
*in*  
**CHEMICAL ENGINEERING**  
**(With Specialization in Industrial Pollution Abatement)**

**By**

**RAKESH KUMAR .D**



**DEPARTMENT OF CHEMICAL ENGINEERING  
INDIAN INSTITUTE OF TECHNOLOGY ROORKEE  
ROORKEE -247 667 (INDIA)  
JUNE, 2010**



INDIAN INSTITUTE OF TECHNOLOGY  
ROORKEE

CANDIDATE'S DECLARATION

---

I hereby declare that the work, which is being presented in the dissertation entitled "ADSORPTIVE DESULFURIZATION USING ACTIVATED CARBON", in the partial fulfillment of the requirements of the award of the degree of Master of Technology in Chemical Engineering with specialization in Industrial Pollution Abatement, submitted in the Department of Chemical Engineering, Indian Institute of Technology Roorkee, Roorkee, Uttarakhand (India), is an authentic record of my own work carried out during the period from June, 2009 to June, 2010 under the supervision of **Dr. V. C. Srivastava**, Assistant professor, Department of Chemical Engineering, Indian Institute of Technology Roorkee, Roorkee.

I have not submitted the matter embodied in this dissertation for the award of any other degree or diploma.

Date: June, 2010

Place: Roorkee

  
(RAKESH KUMAR D.)

---

CERTIFICATE

This is to certify that the above statement made by the candidate is correct to the best of my knowledge and belief.



(Dr. V. C. Srivastava)

Assistant professor,

Department of Chemical Engineering,

Indian Institute of Technology Roorkee,

Roorkee- 247667.

## ACKNOWLEDGEMENT

---

I would like to acknowledge my research guide, **Dr. V. C. Srivastava** for his valuable support and guidance to my dissertation work. He has been a constant source of inspiration to me during my stay at IIT Roorkee. His enthusiastic attitude, innovative ideas and scientific knowledge have inspired me profoundly. It has been an intellectually stimulating and rewarding experience to work with him. I truly feel privileged to have joined under him.

I thank **Dr. I. D. Mall**, Professor & Head, Department of Chemical Engineering, Indian Institute of Technology Roorkee, Roorkee, for his co-operation and suggestions for carrying out this work. It has been a pleasure and a privilege to work with such a talented, perceptive and meticulous Professor.

I am also thankful to Mr. Rajendra Bhatnagar, Technical staff, PARL, Department of Chemical Engineering, for his continuous help provided during my work. I am greatly indebted to Research Scholars Suresh S., J. P. Kushwaha, Sachin Kr. Sharma, and friends and all others for their enthusiastic support, encouragement and help, made me come up with this report.

Finally, I wish to express my sincere thanks to my brother and sisters whose constant support made my work a much easier job. Needless to say that it was because of the efforts of my parents for what I am today.

**(RAKESH KUMAR .D)**

# ABSTRACT

---

Sulfur compounds represent one of the most prevalent impurities found in crude oil. New technologies are required to remove the sulfur from lower quality feed stocks to ensure that energy is available at a reasonable cost. New and more effective approaches and research is required for producing affordable ultra-low-sulfur transportation fuels, to comply with the new government sulfur regulations with maximum sulfur limit of 50 mg/l as per Bharat IV norm. Deep desulfurization of gasoline is restricted largely by dibenzothiophene (DBT), which is the least reactive sulfur compound in gasoline.

The aim of this thesis is to devise a novel desulfurization technique based on adsorption of DBT over commercial activated carbon (CAC) and alum impregnated commercial activated carbon (AMCAC). Characterization of adsorbents was carried out using standard procedures. Scanning electron microscope (SEM), energy dispersive x-ray (EDX), and fourier transform infrared spectroscopy (FTIR) studies were performed to understand the mechanism of oxidation of furfural. Presence of DBT on surface of adsorbents was confirmed by comparison of EDX and XRD of blank and DBT loaded adsorbents.

The parameters studied are initial concentration ( $C_0$ ): 100-900 mg/l; adsorbent dosage (m): 2-22 g/l; time of adsorption (t): 15-735 min; and temperature (T): 10-50 °C. The individual and interactive effects of the above mentioned parameters have been studied using Central Composite Design. Pareto analysis of variance (ANOVA) of the results showed a high coefficient of determination value ( $R^2$  was equal to 0.939 and 0.936 for CAC and AICAC, respectively). Fisher F-value of 16.50 for CAC and 15.92 for AICAC showed satisfactory prediction for second order regression model. Redlich-Peterson isotherm best represented the equilibrium adsorption data. The heat of adsorption and change in entropy for DBT adsorption onto CAC was found to be 9.74 KJ/mol and 85.91 KJ/mol K, respectively. The highest removal of DBT was obtained with  $C_0= 100$  mg/l,  $m= 20$  g/l,  $t= 360$  min and  $T= 30$  °C. AICAC was found to give greater removal of sulfur than CAC.

# CONTENTS

---

	<b>Page No.</b>
<b>CANDIDATE'S DECLARATION</b>	i
<b>ACKNOWLEDGEMENT</b>	ii
<b>ABSTRACT</b>	iii
<b>ABBREVIATIONS</b>	vi
<b>NOMENCLATURE</b>	viii
<b>LIST OF FIGURES</b>	x
<b>LIST OF TABLES</b>	xi

<b>S. No.</b>	<b>Title</b>	<b>Page No.</b>
<b>1.</b>	<b>INTRODUCTION</b>	<b>1-11</b>
	1.1 GENERAL OVERVIEW	1
	1.2 EFFECT ON ENVIRONMENT	2
	1.3 STANDARDS	3
	1.4 GENERAL TECHNIQUES FOR DESULFURIZATION	4
	1.5 ADSORPTION AS A DESULFURIZATION TECHNIQUE	4
	1.6 DIBENZOTHIOPHENE (DBT)	7
	1.7 OBJECTIVE OF THE PRESENT STUDY	8
<b>2.</b>	<b>LITERATURE SURVEY</b>	<b>12-39</b>
	2.1 HYDRODESULFURIZATION (HDS):	12
	2.1.1 RECENT STUDIES IN HDS	13
	2.2 OXIDATIVE DESULFURIZATION (ODS)	18
	2.2.1 RECENT STUDIES IN ODS	19
	2.3 BIODESULFURIZATION (BDS):	24
	2.3.1 RECENT STUDIES IN BDS	24
	2.4 ADSORPTIVE DESULFURIZATION	27
	2.4.1 RECENT STUDIES IN ADSORPTIVE DESULFURIZATION	27

	2.5 IN-SITU PROCESS	32
<b>3.</b>	<b>EXPERIMENTAL PROGRAMME</b>	<b>40-43</b>
	3.1 GENERAL	40
	3.2 CHARACTERIZATION OF ADSORBENTS	40
	3.2.1 X-RAY DIFFRACTION (XRD) ANALYSIS	40
	3.2.2 SCANNING ELECTRON MICROSCOPE (SEM) AND ENERGY DISPERSIVE X-RAY (EDX) STUDY	40
	3.2.3 FOURIER TRANSFORM INFRARED (FTIR)	40
	SPECTROSCOPY	
	3.2.4 PREPARATION OF ALUM IMPREGNATED CAC	41
	3.3 ADSORPTION	41
	3.3.1 ANALYTICAL MEASUREMENT	41
	3.4 CENTRAL COMPOSITE DESIGN	41
	3.5 EXPERIMENTAL PROGRAMME	42
<b>4.</b>	<b>RESULTS AND DISCUSSION</b>	<b>44-69</b>
	4.1 GENERAL	44
	4.2 CHARACTERIZATION OF ACTIVATED CARBON	44
	4.3 CCD ANALYSIS AND FITTING OF SECOND-ORDER POLYNOMIAL EQUATION	45
	4.4 EFFECT OF VARIOUS PARAMETERS ON MO DYE REMOVAL EFFICIENCY	47
	4.4.1 EFFECT OF ADSORBENT DOSAGE (M) AND TEMPERATURE (T)	47
	4.4.2 EFFECT OF INITIAL CONCENTRATION ( $C_0$ ) AND REACTION TIME (T)	48
	4.5 ADSORPTION EQUILIBRIUM STUDY	48
	4.6 ESTIMATION OF THERMODYNAMIC PARAMETERS	50
<b>5.</b>	<b>CONCLUSIONS AND RECOMMENDATIONS</b>	<b>70-71</b>
	5.1 CONCLUSIONS	70
	5.2 RECOMMENDATIONS	70
	<b>REFERENCES</b>	<b>72-81</b>

## ABBREVIATIONS

---

AC	Activated Carbon
ACF	Activated Carbon Fibre
BPy	N-butyl-pyridinium
BT	Benzothiophene
BDS	Biodesulfurization
BiCh	Biocyclohexyl
CA	Carbon Aerosol
CDHDS	Catalytic distillation for desulfurization developed by CDTech
CDHydro	Catalytic distillation for hydrogenation, developed by CDTech
CHB	Cyclohexylbenzene
DBT	Dibenzothiophene
DBT-MO	Dibenzothiophene-monooxygenase
DBTO	Dibenzothiophene-5-oxide, DBT silfoxide
DBTO <sub>2</sub>	Dibenzothiophene-5,5-dioxide, DBT sulfone
DBTO <sub>2</sub> -MO	Dibenzothiophene-5,5-dioxide-monooxygenase
DDS	Direct desulfurization
DEDBT	Diethyle Dibenzothiophene
DEP	Diethylphosphate
DMDBT	DiMethyl Dibenzothiophene
DPS	Diphenylsulfide
EPA	Environmental protection agency
EDF	Equilibrium deposition filtration
FTIR	Fourier Transform Infrared Spectroscopy
GC	Gas Chromatography

HBP	Hydroxybiphenyl
HDS	Hydrodesulfurization
HYD	Hydrogenation
ICE	Intermediate combustion engines
IL	Ionic Liquids
MDBT	Methyl Dibenzothiophene
NA	Napthalene
NO <sub>x</sub>	Oxides of Nitrogen
ODS	Oxidative Desulfurization
PM	Particulate matter
Mg/lw	parts per million by weight
RSH	Thiols
RSR'	Thioethers
SCFB	Standard cubic feet per barrel of liquid feed
SEM	Scanning electron micrograph
SO <sub>x</sub>	sulfur oxidation
SPA-11	Silica-supported phosphoric acid
TH	Thiophene
THDBT	Tetrahydrodibenzothiophene
TMDBT	TriMethyl Dibenzothiophene
XRD	X-ray diffraction



# NOMENCLATURE

---

$1/n$	heterogeneity factor, dimensionless
$a_R$	constant of Redlich-Peterson isotherm, l/mg
$B_T$	Temkin isotherm constant related to the heat of adsorption, kJ/mol
$C_0$	initial concentration of adsorbate in solution, mg/l
$C_e$	equilibrium liquid phase concentration, mg/l
$C_s$	adsorbent concentration in the solution
$I$	constant that gives idea about the thickness of boundary layer, mg/g
$K_F$	constant of Freundlich isotherm, (mg/g)/(l/mg) <sup>1/n</sup>
$K_L$	constant of Langmuir isotherm, l/mg
$K_R$	constant of Redlich-Peterson isotherm, l/g
$K_T$	constant of Temkin isotherm, l/mg
$m$	mass of adsorbent per liter of solution, g/l
$n$	number of data points
$p$	number of parameters
MPSD	Marquardt's percent standard deviation
$q_e$	equilibrium solid phase concentration, mg/g
$q_m$	maximum adsorption capacity of adsorbent as per Langmuir isotherm, mg/g
$q_t$	amount of adsorbate adsorbed by adsorbent at time t, mg/g
R	universal gas constant, 8.314 J/K mol
$t$	time, min
$T$	absolute temperature, K
$V$	volume of the solution, l
$m$	mass of the adsorbent, g
$\Delta G^0$	Gibbs free energy of adsorption, kJ/mol
$\Delta H^0$	enthalpy of adsorption, kJ/mol
$\Delta S^0$	entropy of adsorption, J/K mol

$a_R$	constant of Redlich-Peterson isotherm, l/mg
$\Delta S^0$	initial concentration of each component in solution, mg/l
$a_R$	individual extended Langmuir isotherm constant of each component, l/mg
$C_{0,i}$	number of measurements
$K_i$	number of parameters
$n_m$	number of data points
$n_p$	equilibrium solid phase concentration of each component in binary mixture, mg/g
$q_{e,cal}$	calculated value of solid phase concentration of adsorbate at equilibrium, mg/g
$q_{e,exp}$	experimental value of solid phase concentration of adsorbate at equilibrium, mg/g
$q_{e,cal}$	fraction of the adsorbate adsorbed on the adsorbent under equilibrium

#### Greek symbols

$\beta$	constant of Redlich-Peterson isotherm ( $0 < \beta < 1$ )
$\beta$	constant in SRS model for each component, dimensionless

## LIST OF FIGURES

---

Figure No.	TITLE	Page No.
Fig. 4.1	Scanning electron micrograph of blank and DBT loaded CAC and AICAC.	60
Fig. 4.2(a)	EDX of Blank and DBT loaded CAC	61
Fig. 4.2(b)	EDX of Blank and DBT loaded AICAC	62
Fig 4.3	XRD spectra of blank and DBT loaded CAC	63
Fig. 4.4(a)	FTIR spectra of blank and DBT loaded CAC	64
Fig. 4.4(b)	FTIR spectra of blank and DBT loaded AICAC	64
Fig. 4.5(a)	Normal % probability versus residual error (for CAC).	65
Fig. 4.5(b)	Normal % probability versus residual error (for AICAC).	65
Fig. 4.6(a)	Scatter diagram of predicted response versus actual response for adsorption of DBT onto CAC.	66
Fig. 4.6(b)	Scatter diagram of predicted response versus actual response for adsorption of DBT onto AICAC.	66
Fig. 4.7(a)	3D response graph for DBT removal versus adsorbent dose and temperature (for CAC)	67
Fig. 4.7(b)	3D response graph for DBT removal versus concentration and time (for CAC)	67
Fig. 4.8(a)	3D response graph for DBT removal versus adsorbent dose and temperature (for AICAC)	68
Fig. 4.8(b)	3D response graph for DBT removal versus concentration and time (for AICAC)	68
Fig. 4.9	The van't Hoff plot for the Redlich-Peterson isotherm	69
Fig 4.10	Equilibrium adsorption isotherms at different temperature for DBT CAC system, $t = 6$ h, $C_0 = 50-1000$ mg/l, $m = 20$ g/l. experimental best data points given by the symbols and the lines predicted by Redlich-Peterson equation.	69

## LIST OF TABLES

---

Table No.	TITLE	Page No.
Table 1.1	Sulfur levels in global supplies of crude oil.	09
Table 1.2	Effect of emission norms on pollutants level.	09
Table 1.3	Roadmap of emission standards world over.	10
Table 1.4	Roadmap of Indian emission standards.	10
Table 1.5	Fuel quality specifications for gasoline and diesel.	11
Table 2.1	Removal summary of sulfur by HDS at optimized conditions	34
Table 2.2	Removal summary of sulfur by ODS at optimized conditions.	35
Table 2.3	Removal summary of sulfur by adsorption at optimized conditions	36
Table 2.4	Removal summary of sulfur by adsorption at optimized conditions	38
Table 4.1(a)	Elemental composition of blank and DBT loaded CAC	52
Table 4.1(b)	Elemental composition of blank and DBT loaded AICAC	52
Table 4.2	Process parameters and their levels for Adsorptive desulfurization by using CAC & AICAC	52
Table 4.3(a)	Full factorial design used for Adsorptive desulfurization by using CAC	53
Table 4.3(b)	Full factorial design used for Adsorptive desulfurization by using AICAC	54
Table 4.4(a).	Adequacy of the models tested for desulfurization by CAC.	55
Table 4.4(b).	Adequacy of the models tested for desulfurization by AICAC.	56
Table 4.5(a).	ANOVA for Response Surface Quadratic Model (for CAC).	57
Table 4.5(b).	ANOVA for Response Surface Quadratic Model (for AICAC).	58
Table 4.6	Isotherm parameters for the removal of DBT by CAC (t = 6 h, C <sub>0</sub> = 50-1000 mg/l, m = 20 g/l).	59
Table 4.7	Thermodynamics parameters for the adsorption of DBT by CAC (t = 6 h, C <sub>0</sub> = 50-1000 mg/l, m = 20 g/l).	59

**1.1 GENERAL OVERVIEW**

The demand for transportation fuels has been increasing in most of the countries in the past two decades. The sulfur content in the transportation fuels is a very serious environmental concern. The issues of deep desulfurization are becoming more serious because of the increase in sulfur content of the crude oil and lowering of the regulated sulfur limits in diesel and gasoline. The demand for high-quality, low-sulfur transportation fuels (gasoline, diesel) is growing with increasing concerns related to public health. The combustion of sulfur compounds in fuel oils leads directly to emission of SO<sub>x</sub>, which is not only one of major sources of air pollution and acid rain but also causes many serious diseases of human respiratory system, such as lung cancer. Sulfur emissions also cause respiratory illnesses, aggravate heart disease, trigger asthma, and contribute to formation of atmospheric particulates. The removal of sulfur compounds from petroleum is crucial to producing clean burning fuels. Sulfur compounds poison emission control catalysts and are the source of acid rain. Therefore, more stringent regulations for sulfur in fuel are being implemented by many countries:

However, with this fuel quality, it is difficult to satisfy the practical requirement because the environmental regulations request increasingly low content of sulfur in the ultimate fuel products. In Canada, sulfur reduction under 10 mg/l of “sulfur-free” in diesel fuel by 2005 was recommended. The European Union proposed to reduce the sulfur content in gasoline to maximum 50 mg/l in 2005 and under 10 mg/l of “sulfur-free” gasoline in 2011. The S-content in gasoline will probably reach an average value of about 10 mg/l in many countries by 2010. The sulfur content should also be consistent with international regulations for sulfur in fuel in China. New federal regulations require the removal of sulfur in both gasoline and diesel to very low levels, forcing existing technologies to be pushed into inefficient operating regimes. New technology is required to efficiently produce low sulfur fuels.

Although there are number of organic sulfur compounds present in the fuels, aromatic sulfur compounds such as thiophene (T), benzothiophene (BT), dibenzothiophene (DBT) or methyl substituted dibenzothiophene are of prime concern. Fuels are the largest and most widely

used source of energy in the world. Naturally occurring sulfur compounds left in fuels lead to the emission of sulfur oxide gases. Table 1.1 shows the level of sulfur compounds left in global supplies of crude oil. Sulfur effects these emission control devices by strongly adsorbing to the precious metal catalysts, preventing the adsorption and reaction of hydrocarbons, nitrogen oxides, and carbon monoxide.

Energy generation in a clean and responsible manner can be accomplished in a number of ways. The use non-fossil fuel energy sources such as solar, wind, and nuclear power will eventually replace fossil fuels. However, many of these technologies will require many years before they are able to provide the amounts of energy needed. In the immediate future, fossil fuel-based energy production will continue, and new technologies need to be developed in order to produce clean fuels to power our societies.

It is well known that the sulfur compounds are undesirable in refining process as they tend to deactivate some catalysts used in crude oil processing. Sulfur compounds can cause several corrosion problems in pipeline, pumping, and refining equipments. It may also cause premature failure of combustion engines and poisoning of the catalytic converters that are used automotive engines. Sulfur compounds exist in various forms and can be classified into four main groups: mercaptants, sulfides, disulfides and thiophenes. Due to the chemistry of sulfur compounds (oxidation of sulfur compounds produce oxides of sulfur, while reduction of S compounds produce  $H_2S$ ), catalytic converters cannot be used to board a vehicle to reduce its negative impact. Therefore, it is better to produce low sulfur fuels for our well-being and environmental protection.

The removal of DBT by adsorption with activated carbon is presented in this thesis. This method reduces the level of one sulfur compound to  $< 20$  mg/l from 100 mg/l by weight sulfur by selectively adsorption of DBT compound.

## **1.2 EFFECT ON ENVIRONMENT**

Pollution caused by combustion engines contribute greatly to the air quality problems worldwide. Sulfur compounds get converted to sulfur oxides by combustion, and these ultimately lead to acid rain [Koch et al., 1996, Whitehurst et al., 1998]. Even with more stringent

Table 1.5 shows the journey of emission standards in India, and Table 1.6 shows the fuel specifications for gasoline fuels as per various Bharat-Stage norms in India the latest regulations in India to reduce the gasoline sulfur content from current maximum of 150 mg/l to 50 mg/l by 2010, and cut the diesel sulfur content from current 350 mg/l to 15 mg/l by 2010, refineries are facing major challenges to meet the fuel sulfur specification along with the required reduction of aromatics contents.

#### **1.4 GENERAL TECHNIQUES FOR DESULFURIZATION**

HDS is the most commonly used method of sulfur reduction of fossil fuels in refineries. Typically, it involves catalytic treatment with hydrogen to convert the various sulfur compounds to hydrogen sulfide [Chan et al., 2000, Nikkolaj et al., 2000]. HDS requires application of severe operating conditions and the use of especially activated catalysts for the production of fuels with the very low levels of sulfur compounds [Michael and Bruce, 1991; Heeyon et al., 2003]. HDS is however, limited in treating benzothiophenes (BTs) and DBTs, especially DBTs having alkyl substituent on 4 and/or 6 positions. Moreover, the HDS process has reached a stage where increasing temperature and pressure are just enough to remove last traces of sulfur without affecting the octane number. Some prominent level desulfurization techniques under investigation are oxidative desulfurization (ODS), Bio desulfurization (BDS) and adsorption. Detailed review about all these methods is given in chapter 2.

#### **1.5 ADSORPTION AS A DESULFURIZATION TECHNIQUE**

Adsorption is a surface phenomenon. The material adsorbed is called the adsorbate or solute and adsorbing phase is the adsorbent. In the water purification, adsorbents are used to remove organic impurities, particularly those are non-biodegradable or associated with taste, colour, and odour. Although adsorption is applied in low concentration, recent physical-chemical processes use adsorption as a primary technique to remove soluble organic from wastewater. The adsorption is called physical when relatively weak intermolecular forces cause the attachment and chemical, when chemical bonding like forces, causes this attachment. During adsorption, the solid adsorbent becomes saturated or nearly saturated with the adsorbate. To recover the

adsorbate and allow the adsorbent to be reused, it is regenerated by desorbing the adsorbed substance (i.e. the adsorbates).

Adsorption process can be classified as either physical adsorption (van der Waals adsorption) or chemisorptions (activated adsorption) depending on the type of forces between the adsorbate and adsorbent, in physical adsorption, the individuality of the adsorbate and the adsorbent are preserved. In chemisorptions, there is a transfer or share of electron, or breakage of the adsorbate into atoms or radicals, which are bound separately.

Physical adsorption occurs quickly and may be monomolecular (unimolecular) layer on monolayer, or two, three or more layers thick (multi-molecular). As physical adsorption takes place, it begins as a monolayer. It can then become multi-layer, and then, if the pores are close to the size of the molecules, more adsorption occurs until the pores are filled with adsorbate. Accordingly, the maximum capacity of a porous adsorbent can be more related to the pore volume than the surface area. In contrast, chemisorption is monolayer, involves the formation chemical bonds between the adsorbent and adsorbate.

Most commercial adsorbents rely on physical adsorption; while catalyst relies on chemisorptions.

In the adsorptive desulfurization technique, the active adsorbent is placed on a porous, non-reactive substrate that allows high surface area for the adsorption of sulfur compounds. Adsorption occurs when the sulfur molecules attach to the adsorbent and remain there separate from the fuel. Various investigators have utilized this technique for the removal of sulfur from various types of fuels and model oils by various types of adsorbents [Weitkamp et al., 1991; Lee et al., 2002; Ma et al., 2002; Lu, 2000; Mckinley, 2003; Hernandez and Yung 2004; Haji, 2005; Sano et al., 2005; Gongshin, 2006; Li et al., 2007]. Desulfurization by adsorption faces the challenge of developing easily remunerable adsorbent with a high adsorption capacity. Adsorbents developed must have high selectivity for the adsorption of refractory aromatic sulfur compounds that do not get removed during the HDS process.

Activated carbon has an extraordinarily large surface area and pore volume that gives it a unique adsorption capacity [Baker et al., 1992]. Commercial grade products range between 300



and 2,000 m<sup>2</sup>/g [Burdock, 1997]. Some have surface areas as high as 5000 m<sup>2</sup>/g. The specific mode of action is extremely complex, and has been the subject of much study and debate. Activated carbon has good adsorptive properties and has been used for the removal of organic compound from aqueous solutions [Marko et al., 2003]. Activated carbon has both chemical and physical effects on substances where it is used as a treatment agent. Activity can be separated into (1) adsorption; (2) mechanical filtration; (3) ion exchange; and (4) surface oxidation.

In a recent study, Muzic et al. [2010] studied removal of sulfur from diesel fuel by adsorption on a commercial activated carbon and 13X type zeolite in a batch adsorber. Kinetic characterization of the adsorption process was performed applying Lagergren's pseudo-first order, pseudo-second order and intraparticle diffusion models using data collected during experiments carried out to determine the sulfur adsorption dependency on time. The experiments investigating adsorption efficiency regarding initial sulfur concentration were also performed and the results were fitted to Langmuir and Freundlich isotherms, respectively. Activated carbon Norit SXRO PLUS was found to have much better adsorption characteristics. The process of sulfur adsorption on the fore mentioned activated carbon was further studied by statistically analyzing data collected during experiments which were carried out according to three-factor two-level factorial design. Statistical analysis involved the calculation of effects of individual parameters and their interactions on sulfur adsorption and the development of statistical models of the process.

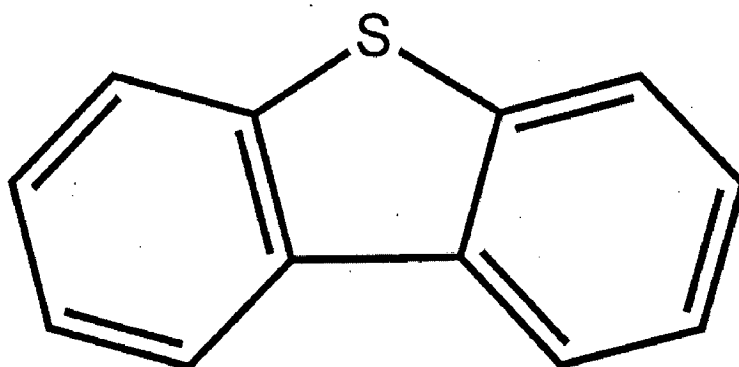
Kim et al. [2005] studied the adsorptive desulfurization using a model diesel fuel over three typical adsorbents (activated carbon, activated alumina and nickel-based adsorbent) in a fixed-bed adsorption system. To date, no work is available in literature on the utilization of activated carbon for the adsorptive treatment of DBT bearing model oil. Also, very few adsorption studies on desulfurization focused on the engineering aspects like isotherm and thermodynamics of the adsorption process that are important in designing adsorption system. No attempt was made to optimize the parameters for maximum removal efficiency using Response Surface Methodology.

## 1.6 DIBENZOTHIOPHENE (DBT)

### 1.6.1 Properties

Molecular formula	$C_{12}H_8S$
Molar mass	184.26 g/mol
Appearance	Colourless crystals
Density	1.252 g/cm <sup>3</sup>
Melting point	97-100 °C (lit.)
Boiling point	332-333 °C
Solubility in water	insol.
Solubility in other solvents	benzene and related

### 1.6.2 Structure of DBT



## 1.7 OBJECTIVES OF THE PRESENT STUDY

The objective of this study is to investigate removal of sulfur from model oil (dibenzothiophene (DBT) dissolved in iso-octane) using commercial activated carbon (CAC) and alum impregnated commercial activated carbon (AICAC) as adsorbents. The objectives of the present study are:

1. To carry out detailed characterization of CAC and AICAC, before and after adsorption of DBT so as to understand the adsorption mechanism. These characteristics include X-ray diffraction (XRD), scanning electron micrograph (SEM), Fourier transform infrared (FTIR) spectroscopy and energy dispersive X-ray (EDX) spectra.
2. To study and optimize the effect of initial concentration ( $C_0$ ), adsorbent dosage ( $m$ ), time of adsorption ( $t$ ), and temperature ( $T$ ) for the removal of DBT by CAC and AICAC using the central composite design.
3. To study the equilibrium sorption behavior of the adsorbents using the adsorption isotherm technique, and to determine the best isotherm to correlate the experimental data.
4. To study the thermodynamics of the adsorption process by finding out changes in Gibbs free energy, enthalpy and entropy.

**Table 1.1 Sulfur levels in global supplies of crude oil.**

Region	Crude Oil gravity (API)	Sulfur weight (% ,1990)	Production (tpd)	Crude Oil gravity (API)	Sulfur weight (% ,2010)	Production (tpd)
Alaska	26.970	1.11	1,954	28.340	0.99	1,645
Canada	31.400	1.52	2,000	32.000	1.62	2,500
California	17.430	1.59	970	18.730	2.60	951
Rest of USA	35.110	0.86	4,510	36.930	0.88	2,470
Africa	31.280	0.17	7,000	32.640	0.18	6,100
Europe	33.200	1.09	16,330	33.700	1.10	15,530
Latin America	25.060	1.62	7,770	27.100	1.82	9,850
Middle East	33.730	1.69	29,100	34.350	1.71	35,760
Far East	33.800	1.09	16,330	37.300	1.10	15,530
World Average	31.300	1.13	70,800	32.810	1.27	83,450

Source: United Nations Environment Program, 2006

**Table 1.2 Effect of Emission Norms on pollutants level.**

Vehicle Type		Emission Reduction on 10 mg/l sulfur fuels relative to fuels with 500 mg/l (%)			
		CO <sub>2</sub>	NO <sub>x</sub>	HC <sub>s</sub>	PM
Euro IV cars	Petrol	3	0	0	0
	Diesel	2	0	0	0
Euro I, II, III cars	Petrol	0	10	10	0
	Diesel	0	0	0	5
Euro IV vans	Petrol	0	0	0	0
	Diesel	2	0	0	0
Euro I, II, III vans	Petrol	0	10	10	0
	Diesel	0	0	0	5
Euro IV HDVs	Diesel	2	0	0	0
Euro I, II, III HDVs	Diesel	0	0	0	5

Source: United Nations Environment Program, 2006

**Table 1.3 Roadmap of Emission standards world over.**

Country	96	97	98	99	00	01	02	03	04	05	06	07	08	09	10
<b>California (US)</b>	CARB (90 mg/l)			CARB (80 mg/l)					CARB (15 mg/l)						
<b>USA</b>	EPA (500 mg/l)							300 mg/l	80 mg/l	15 (mg/l)					
<b>EU</b>	Euro II (500 mg/l)				E III (150 mg/l)			E IV 50 mg/l		E V 10 mg/l					
<b>China(H)</b>	E1	Euro II			Euro III				Euro IV						
<b>Thailand</b>	Euro I			E II		Euro III			E IV						
<b>Singapore</b>	Euro I			E II		Euro III			E IV						
<b>Malaysia</b>	Euro I			Euro II					E III						
<b>India (metros)</b>	E I		Euro II				Euro III			E IV					
<b>India</b>	Euro I			Euro II			Euro III			E III					
<b>Nepal</b>	Euro I														
<b>Philippines</b>	Euro I														
<b>Indonesia</b>	Euro II														

Source: Modified from CAI-Asia, 2006

**Table 1.4 Roadmap of Indian emission standards.**

Standard	Reference	Date	Region
<b>India 2000</b>	Euro 1	2000	Nationwide
<b>Bharat Stage II</b>	Euro 2	2001	NCR*, Mumbai, Kolkata, Chennai
		April, 2003	NCR*, 12 Cities†
		April, 2005	Nationwide
<b>Bharat Stage III</b>	Euro 3	April, 2005	NCR*, 12 Cities†
		April, 2010	Nationwide
<b>Bharat Stage IV</b>	Euro 4	April, 2010	NCR*, 12 Cities†

Source: Kalhe, 2006

\* National Capital Region (Delhi)

† Mumbai, Kolkata, Chennai, Bengaluru, Hyderabad, Ahmedabad, Pune, Surat, Kanpur, Lucknow, Sholapur, and Agra

**Table 1.5 Fuel quality specifications for gasoline and diesel.**

<b>Standard</b>	<b>Gasoline</b>		<b>Diesel</b>			
	<b>Lead (mg/l)</b>	<b>Benzene (%)</b>	<b>Sulfur (mg/l)</b>	<b>Sulfur (mg/l)</b>	<b>Cetane Number</b>	<b>Density (kg/m<sup>3</sup>)</b>
<b>India 2000</b>	130	3(Metros) 5(Rest of India)	1000	2500	48	820-860
<b>Bharat Stage II</b>	130	3(Metros) 5(Rest of India)	500	500	48	820-860
<b>Bharat stage III</b>	50	1	150	350	51	820-845
<b>Bharat stage IV</b>	50	1	50	50	51	820-845

Source: Jindal, 2004

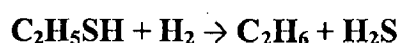
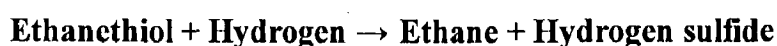
## 2.1 HYDRODESULFURIZATION (HDS):

Hydro-desulfurization (HDS) is a catalytic chemical process widely used to remove sulfur (S) from natural gas and from refined petroleum products such as gasoline or petrol, jet fuel, kerosene, diesel fuel, and fuel oils. The purpose of removing the sulfur is to reduce the sulfur dioxide (SO<sub>2</sub>) emissions that result from using those fuels in automotive vehicles, aircraft, railroad locomotives, ships, gas or oil burning power plants, residential and industrial furnaces, and other forms of fuel combustion [Selvavathi et al., 2009].

Another important reason for removing sulfur from the naphtha streams within a petroleum refinery is that sulfur, even in extremely low concentrations, poisons the noble metal catalysts (platinum and rhenium) in the catalytic reforming units that are subsequently used to upgrade the octane rating of the naphtha streams.

The industrial hydrodesulphurization processes include facilities for the capture and removal of the resulting hydrogen sulfide (H<sub>2</sub>S) gas. In petroleum refineries, the hydrogen sulfide gas is then subsequently converted into by product elemental sulfur. In fact, the vast majority of the 64,000,000 metric tons of sulfur produced worldwide in 2005 was by product sulfur from refineries and other hydrocarbon processing plants. An HDS unit in the petroleum refining industry is also often referred to as a Hydrotreater [Wangliang et al., 2009].

Hydrogenation is a class of chemical reactions in which the net result is the addition of hydrogen (H). Hydrogenolysis is a type of hydrogenation and results in the cleavage of the C-X chemical bond, where C is a carbon atom and X is a sulfur, nitrogen (N) or oxygen (O) atom. The net result of a hydrogenolysis reaction is the formation of C-H and H-X chemical bonds [Selvavathi et al., 2009]. Thus, Hydrodesulfurization is a hydrogenolysis reaction. Using ethanethiol (C<sub>2</sub>H<sub>5</sub>SH), a sulfur compound present in some petroleum products, as an example, the hydrodesulphurization reaction can be simply expressed as



### 2.1.1 Recent studies in HDS

Farag et al. [2000] studied the Hydrodesulfurization (HDS) reactions of dibenzothiophene (DBT) and 4,6-dimethyldibenzothiophene (4,6-DMDBT) over synthesized CoMo-based carbon catalysts and CoMo/ Al<sub>2</sub>O<sub>3</sub> commercial catalyst using a sampling micro-autoclave reactor at 300-380 °C and 2.9 MPa hydrogen initial pressure. They observed that CoMo-based carbon catalysts showed higher activity than CoMo/ Al<sub>2</sub>O<sub>3</sub> commercial catalyst. The HDS selectivity of DBT in terms of direct de-sulfurization and hydrogenation routes was found to be almost independent of the temperature, whereas a dramatic change with 4,6-DMDBT was observed on both catalysts. The presence of 10 wt% naphthalene during the HDS of dibenzothiophene was found to inhibit both direct de-sulfurization and hydrogenation routes, while self-produced H<sub>2</sub>S inhibited only the direct de-sulfurization. Excess slightly reduced the rate of hydrogenation reaction as well. The trend of inhibition by naphthalene was similar for both CoMo-based carbon and CoMo/Al<sub>2</sub>O<sub>3</sub> catalysts. However, much more inhibition by H<sub>2</sub>S was observed with carbon support. Based on the kinetic analysis of inhibition, active sites on CoMoS for de-sulfurization and hydrogenation are discussed.

Shafi et al. [2000] proposed that silica-supported monometallic tungstophosphoric heteropoly acid (HPA), H<sub>3</sub>PW<sub>12</sub>O<sub>40</sub>, is a novel and efficient catalyst for the hydrodesulfurization of dibenzothiophene (DBT). They observed that over a 30 wt.% HPA/SiO<sub>2</sub> catalyst in a trickle bed flow reactor at industrially relevant gas and liquid space velocities (GHSV 600 h<sup>-1</sup> and LHSV 6 h<sup>-1</sup>) and an H<sub>2</sub> pressure of 30 bar, the hydrodesulfurization proceeds with a DBT conversion of 58% at 290 °C and 80% at 350 °C. These values are comparable to the performance of the industrial Co-Mo/Al<sub>2</sub>O<sub>3</sub> catalyst. No loss of catalytic activity was observed for a period of 56 h. 31P MAS NMR and thermogravimetric analysis (TGA) data show that the HPA decomposes upon interaction with H<sub>2</sub>S /H<sub>2</sub> to yield the active hydrodesulfurization catalyst.

Kwak et al. [2000] tested CoMoS/Al<sub>2</sub>O<sub>3</sub> catalysts containing different amounts of fluorine for the hydrodesulfurization (HDS) of dibenzothiophene (DBT), 4-methyldibenzothiophene (4-MDBT), and 4,6-dimethyldibenzothiophene (4,6-DMDBT), and the results have been analyzed based on three fundamental reactions involved in the HDS mechanism: hydrogenation of the aromatic ring, hydrogenolysis of the C-S bond, and migration of methyl groups in the ring structure. They proposed that fluorine addition to the catalyst



promotes all of these three reactions due to the enhancement of two factors: the metal dispersion and the catalyst acidity. The extents that the HDS rates are improved by fluorine addition increase in the order of DBT < 4-MDBT < 4,6-DMDBT. Product distributions change in characteristic trends with fluorine addition depending on the individual reactants. That is, in DBT HDS, CHB obtained by the ring saturation is enhanced more than BP produced by the direct desulfurization, while the opposite trend is observed in 4-MDBT HDS. 4,6-DMDBT HDS shows an intermediate trend: products of both types are promoted to similar extents on fluorinated catalysts. They reported that the migration of methyl groups in the reactant ring structure due to the catalyst acidity, which reduces the steric hindrance to the C–S bond, is responsible for the characteristic trends in the product distribution observed with the individual reactants.

Kabe et al. [2001] studied the effects of the H<sub>2</sub>S partial pressure on the catalytic activity and product selectivity of the hydrodesulfurization (HDS) reactions of dibenzothiophene (DBT) and 4,6-dimethyldibenzothiophene (4,6-DMDBT) were investigated over the sulfided NiMo/Al<sub>2</sub>O<sub>3</sub> and NiW/Al<sub>2</sub>O<sub>3</sub> catalysts under the deep desulfurization conditions (sulfur concentrations < 0.05 wt.%). The inhibiting effects of H<sub>2</sub>S were observed in the HDS reactions of both DBT and 4,6-DMDBT. The HDS reaction of DBT was more strongly inhibited by H<sub>2</sub>S than that of 4,6-DMDBT over each catalyst. The formations of both biphenyls (BPs) and cyclohexylbenzenes (CHBs) were inhibited by H<sub>2</sub>S, but the former were inhibited more strongly. The NiMo/Al<sub>2</sub>O<sub>3</sub> catalyst was less susceptible to the inhibiting effect of H<sub>2</sub>S than the NiW/Al<sub>2</sub>O<sub>3</sub> catalyst. The promotion of Ni on NiMo catalyst reduced the inhibiting effect of H<sub>2</sub>S on the HDS activity. The HDS reactions were expressed by the Langmuir–Hinshelwood rate equation to examine the mechanisms of the inhibiting effects of H<sub>2</sub>S over the various catalysts. Over each catalyst, the heats of adsorption increased in the order DBT < 4,6-DMDBT < H<sub>2</sub>S. Since H<sub>2</sub>S was adsorbed on the catalyst more strongly than DBTs, the HDS reactions of DBTs were inhibited.

Vargas-Villamil et al. [2004] developed a light gas oil hydrodesulfurization process via catalytic distillation and compared to a conventional process. They proposed that by integrating the separation and reaction into a single unit, the catalytic distillation may produce a diesel with low concentration of sulfur compounds at a lower cost than the traditional reaction/separation process. The process proposed in this work is compared to an optimized conventional

hydrodesulfurization unit which represents fairly well a plant that belongs to the National System of Refineries. During the optimization of the conventional process, a compromise is established among the production of diesel and naphtha and the operating costs. The results show that the light gas oil hydrodesulfurization via catalytic distillation is as or more efficient than the conventional process. However, the removal of the sulfur compounds is carried out under less rigorous conditions. This design reduces the fix and operational costs.

Siliceous MCM-41-supported nickel phosphides from a precursor with a Ni/P atomic ratio of 3, 2, 1.25, 1, 0.5, or 1/3 were prepared by in situ reduction. Wang et al. [2005] used a high heating rate and a multistep program to prepare the supported nickel phosphides. The in situ reduction method proved superior to the traditional reduction–passivation–reduction method. The timely removal of local moisture from the surface during reduction is crucial to obtaining a high hydrodesulfurization (HDS) performance of the phosphide catalysts. The precursors were characterized by TPR to investigate the reactions involved in phosphide preparation, and the structures of the resulting nickel phosphides were characterized by means of P NMR and XRD. Nickel phosphide formation may start with the reduction of NiO to Ni, and the Ni metal may assist phosphide formation in the reduction of nickel-rich precursors. They reported that Nickel-rich phosphides exhibited much higher HDS activity than phosphorus-rich phosphides prepared by the in situ reduction method. Reduction of the precursor with Ni/P = 2 yielded Ni<sub>12</sub>P<sub>5</sub>/MCM-41, whereas reduction of the precursor with Ni/P = 1.25 produced Ni<sub>2</sub>P/MCM-41. As in the traditional reduction–passivation–reduction method, a small excess of phosphorus in the precursors is also needed to obtain the desired nickel-rich phosphides by the in situ reduction method. Ni<sub>2</sub>P/MCM-41 was the most active catalyst in the HDS of dibenzothiophene among all of the supported nickel phosphides prepared by the in situ reduction method.

Bionda et al. [2005] studied the influence of some reaction parameters on hydrodesulfurization (HDS) in the experimental trickle-bed reactor (Andreas–Hofer apparatus). A mixture of two gas oils (atmospheric gas oil and light cyclic oil from FCC) was used as feed. The investigations were performed at 300 °C, under space velocity from 1.0 to 2.5 m<sup>3</sup>/m<sup>3</sup> h, hydrogen pressure of 40 and 65 bar, at H<sub>2</sub>/CH ratio from 100 to 500. A simple reactor and a kinetic model were used, yielding good agreement between experimental and theoretical values of sulfur concentrations. Simulation experiments were performed by changing H<sub>2</sub>/CH ratio,

pressure and LHSV. The correlation recorded between the changed parameters and sulfur content was in that with higher pressure and ratio of  $H_2/CH$  the percentage of removed sulfur increased. Increased space velocity produced opposite effect. These experimental results and the change of either one or more process parameters or of the catalyst type enabled performance of the industrial reactor.

Wang et al. [2008] synthesized two intermediates of dibenzothiophene (DBT)—tetrahydro-DBT (THDBT) and hexahydro-DBT (HHDBT), and their hydrodesulfurization (HDS) mechanism was investigated over  $Mo/\gamma-Al_2O_3$  at 300–340 °C and 5 MPa in the absence and presence of  $H_2S$  and 2-methylpiperidine. The rate constants of all steps in the kinetic network of the HDS of DBT were measured. THDBT underwent desulfurization by hydrogenolysis to 1-phenylcyclohexene, followed by hydrogenation to phenylcyclohexane. The desulfurization of HHDBT occurred by hydrogenolysis of the aryl C–S bond and then cleavage of the cycloalkyl C–S bond of the resulting thiol by elimination to 1-phenylcyclohexene and by hydrogenolysis to phenylcyclohexane. From their studies they concluded that  $H_2S$  strongly inhibited the desulfurization of all three molecules but did not inhibit (de)hydrogenation. 2-Methylpiperidine also had a strong inhibitory effect, especially on (de)hydrogenation and, to a lesser extent, on desulfurization. The order of the inhibition of DBT, THDBT, and HHDBT was explained by the adsorption constants of these three molecules.

Xiang et al. [2008] investigated the influence of indole on the hydrodesulfurization (HDS) of dibenzothiophene (DBT) and the influence of DBT on the hydrodenitrogenation (HDN) of indole over a presulfided  $NiMoS/\gamma-Al_2O_3$  catalyst in a fixed-bed high-pressure microreactor. A significant negative effect of indole on the HDS of DBT was observed. They reported that the inhibitory effect of indole on the hydrogenation route (HYD) was stronger than on the direct desulfurization route (DDS). Indole and its HDN intermediate products suppressed HDS of DBT through the competitive adsorption on active sites of the catalyst. DBT and  $H_2S$  produced in situ promoted the conversion of coordinatively unsaturated sites (CUS) to Bronsted acid sites on the catalyst surface, which in turn facilitated the cleavage of  $C(sp^3)$ -N bond in indoline; the conversion of indole and the relative concentration of *o*-ethylaniline (OEA) then increased. They came up with the conclusion that although the presence of sulfur atoms is essential for the formation of active sites on the catalyst for HDN, a small amount of sulphur

species is sufficient to maintain the HDN active sites; higher content of sulfides may bring on a negative influence on the HDN of indole.

Wang et al. [2009] determined the rate constants of all reaction steps in the hydrodesulfurization (HDS) of dibenzothiophene (DBT), 4,6-dimethyldibenzothiophene (DMDBT), and their tetra- and hexahydro intermediates TH(DM)DBT and HH(DM)DBT over Ni-MoS<sub>2</sub>/c-Al<sub>2</sub>O<sub>3</sub>. DBT, THDBT, DMDBT, and THDMDBT underwent desulfurization by hydrogenolysis of both C-S bonds, while HHDBT and HHDMDBT underwent desulfurization by cleavage of the aryl C-S bond by hydrogenolysis, followed by cleavage of the cycloalkyl C-S bond by elimination as well as by hydrogenolysis. Ni promoted the C-S bond breakage of DBT, THDBT, and HHDBT strongly, but promoted the (de)hydrogenation only weakly. The methyl groups suppressed the desulfurization in the order DMDBT > THDMDBT > HHDMDBT and promoted hydrogenation. They reported that these different degrees of steric hindrance are due to the hydrogenation of a phenyl ring, which makes the THDBT and HHDBT rings flexible. H<sub>2</sub>S strongly inhibited the desulfurization rates in the order (DM)DBT > TH(DM)DBT > HH(DM)DBT, but inhibited the (de)hydrogenation rates only lightly. 2-Methylpiperidine inhibited the hydrogenation of all molecules.

The need for more complete removal of sulphur from fuels is due to the lower allowable sulphur content in gasoline and diesel, which is made difficult by the increased sulphur contents of crude oils. Deng et al. [2010] reported an experimental study on the hydrodesulfurization (HDS) of diesel in a slurry reactor. HDS of straight-run diesel using a NiMoS/Al<sub>2</sub>O<sub>3</sub> catalyst was studied in a high-pressure autoclave for the following operating conditions: 4.8–23.1wt% catalyst in the reactor, 320–360 °C, 3–5MPa pressure, and 0.56–2.77 L/min hydrogen flow rate. It was found that the reaction rate was proportional to the catalyst amount and increased with temperature, pressure and hydrogen flow rate. The reaction kinetics for the HDS reaction in the slurry reactor was obtained. As compared with HDS in a fixed bed reactor, HDS in a slurry reactor is promising because of the uniform temperature profile, high catalyst efficiency, and online removal and addition of catalyst.

## 2.2 OXIDATIVE DESULFURIZATION (ODS):

The key feature of the oxidative desulfurization process is the complementary chemistry to hydrodesulphurization. In fact, the most refractory compounds to hydrodesulfurize are the dibenzothiophenes which, on the contrary, show the highest oxidation rate in the oxidative desulfurization [Xiaoliang et al., 2007]. Oxidative desulfurization is a good fit as a finishing process downstream of an existing hydrodesulphurization unit (HDS) producing 300-500 wmg/l S.

There are several oxidative desulfurization technologies available.

- A general process consists of three sections:
- A peroxide supply section,
- A sulfone generation section and
- A sulfone separation section.

The first section comprises all the peroxide storage and handling facilities. In the second stage the hydrotreated diesel is mixed with the oxidant and the mixture contacted with an oxidation catalyst active for oxidation of sulfur compounds [Wangliang et al., 2009]. The oxidation reaction causes physical-chemical properties of the sulfur compounds to significantly change [Xiaoliang et al., 2007]. Taking advantage of this change, it is simple in the final step of the process to separate oxidation products from the diesel stream by using either solvent extraction or adsorption.

The advantages of the oxidative desulfurization process can be summarized as follows:

1. Does not use hydrogen to produce ULSD
2. Mild operating conditions
3. Complementary chemistry to hydrodesulphurization
4. Use conventional reaction and separation refinery equipments
5. Flexibility to process cracked feed stocks.

Oxidative Desulfurization (ODS) as an alternative process to the traditional processes has received much attention for deep desulfurization of fuels for a number of reasons [Dehkordi et al., 2009]. This is because the ODS process has two main advantages compared to the HDS process [Bagreev et al., 2005]. First, the greatest advantage of the ODS process is that it can be carried out in the liquid phase and under very mild operating conditions. Second, the most refractory sulfur-containing compounds to the HDS process, (e.g., DBT and its derivatives) show high reactivity toward the oxidation by this method.

According to the ODS process, these refractory sulfur compounds are oxidized to their corresponding sulfoxides and subsequently sulfones [Dehkordi et al., 2009]. Afterward, these highly polarized products can be removed by a number of separation processes including solvent extraction, adsorption, etc.

Various types of oxidants and catalysts have been examined for the ODS process. Oxidants used include hydrogen peroxide, nitric acid, nitrogen oxides, organic hydro peroxides (e.g., tert-butyl hydro peroxide), ozone, oxygen, etc. Hydrogen peroxide is the most widely used oxidant because it is environmentally friendlier [Wangliang et al., 2009]. Hydrogen peroxide in the presence of catalysts such as acetic acid, formic acid and polyoxometalate has been used. However, different solid basic catalysts such as polymolybdates supported on alumina,  $V_2O_5/Al_2O_3$  and  $V_2O_5/TiO_2$ , and Co-Mo/ $Al_2O_3$  have been also used.

The main reasons for the use of hydrogen peroxide as oxidizing agent are:

- (1) Its low cost,
- (2) Non-polluting,
- (3) Non strongly corrosive, and
- (4) Commercial availability.

### **2.2.1 Recent studies in ODS**

Jeyagowry et al. [2006] has been demonstrated that Mn- and Co-containing oxide catalysts are highly effective for selective oxidation of the refractory sulfur compounds in diesel fuel using molecular oxygen in air at atmospheric pressure and the sulfur content can be easily reduced to 40–60 mg/l after coupled with extraction by polar solvent. In this system, the catalyst (heterogeneous) can be easily reactivated and reused. The low-sulfur (10–15 mg/l sulfur) diesel

was obtained by simply pass through treated diesel (oxidized and solvent extracted diesel) into the activated basic  $\gamma$ - $\text{Al}_2\text{O}_3$  adsorbent-bed at room temperature. Oxidative desulfurization process which they performed has several advantages over other oxidative desulfurization processes which were reported. One advantage of this process that the reaction can be carried out using inexpensive oxygen found air compare to costly oxidants, such as  $\text{H}_2\text{O}_2$  or ozone, which were reported in the literature for the oxidative desulfurization processes. In addition, the use of air as oxidant also eliminates the need to carry out any oxidant recovery process that is usually required if liquid oxidants (tert-butylperoxide or  $\text{H}_2\text{O}_2$ ) are used. Another advantage of this process is the mild operating conditions compared to hydrodesulfurization process which more severe conditions are needed.

Yongchuan et al. [2008] studied an oxidative desulfurization method using ultrasound/Fenton's reagent. Using the hydrotreated Middle East diesel fuel as a feedstock, four processes of the oxidative desulfurization have been studied: a hydrogen peroxide–acetic acid system and a Fenton's reagent system both without/with ultrasound. The results showed that the total sulfur removal rate of diesel fuels increases with the increasing of the ultrasonic power. The combination of ultrasound and supplementary Fe (II) desulfurization of the hydrotreated diesel fuel are more rapid than either sonication or Fenton's reagent alone. The Fenton's reagent improves the hydrotreated diesel fuel desulfurization rate in this study, probably by increasing the concentration of available -OH. The total sulfur content of hydrotreated Middle East diesel fuel can decrease from 568.75  $\mu\text{g/g}$  to 9.50  $\mu\text{g/g}$ . It satisfies the new regulation requiring about use of low-sulfur diesel fuels. Hence, they reported that oxidative desulfurization technology using the ultrasound–Fenton's reagent system that integrating HDS can be used to product low-sulfur diesel fuels and/or ultra-low sulfur diesel fuels.

Antonio et al. [2006] studied oxidative desulfurization (ODS) of model sulfur-containing compounds (thiophene, 2-methylthiophene, benzothiophene, 2-methylbenzothiophene, dibenzothiophene, 4-methyldibenzothiophene, and 4, 6-dimethyldibenzothiophene) with tert-butyl hydroperoxide on different metal containing molecular sieves. It allowed studying the role of electronics and geometry of the reactant as well as the pore dimensions, topology, and adsorption properties of the catalyst on the rate of desulfurization. The best catalysts were then studied for the ODS of simulated and industrial diesel in a continuous fixed-bed reactor.

MoO<sub>x</sub>/Al<sub>2</sub>O<sub>3</sub> catalysts were active, but rapid deactivation occurs due to metal leaching and sulfone adsorption. Calcined Ti-MCM-41 was more active, did not leach Ti, and deactivated more slowly than MoO<sub>x</sub>/Al<sub>2</sub>O<sub>3</sub>. They reported that the amount of adsorbed sulfone was strongly reduced by decreasing the polarity of the Ti-MCM-41 by silylation, with the corresponding increase in catalyst activity and lifetime.

Zhao et al. [2009] conducted experiments to examine desulfurization of dibenzothiophene using acidic ionic liquid. The oxidative desulfurization of dibenzothiophene (DBT) in *n*-octane as model oil with Brønsted acidic ionic liquids (ILs) N-methyl-pyrrolidonium phosphate (H<sub>2</sub>PO<sub>4</sub>) as catalytic solvent and H<sub>2</sub>O<sub>2</sub> as oxidant was optimized by orthogonal experiments. 99.8% of DBT in the model oil was removed under the optimal conditions of molar ratio of H<sub>2</sub>O<sub>2</sub> to sulfur of 16: 1, reaction temperature of 60 °C, reaction time of 5 h, and volume ratio of model oil to ILs of 1: 1. The desulfurization efficiency of actual diesel was 64.3% under the optimized conditions. The influences of the desulfurization efficiency of DBT decreased in the following order: oxidation temperature > oxidation time > molar ratio of H<sub>2</sub>O<sub>2</sub>/sulfur (O/S) > volume ratio of H<sub>2</sub>PO<sub>4</sub> to model oil (*V*<sub>IL</sub>/*V*<sub>model oil</sub>). The IL H<sub>2</sub>PO<sub>4</sub> can be recycled six times without a significant decrease in activity.

Prasad et al. [2008] prepared alumina, silica–alumina and magnesia–alumina supported, unpromoted and bismuth promoted 15 wt.% molybdenum oxide catalysts and characterized by XRD, surface area and oxygen chemisorption. The catalysts were evaluated for the oxidative desulfurization (ODS) of 4,6-dimethyl dibenzothiophene to the corresponding sulfone using tert-butyl hydroperoxide as oxidant. Among all the catalysts examined, Bi-Mo/Siral 1 exhibited the best catalytic performance compared to all the catalysts examined. The catalyst also showed high conversion with appreciable stability until 300 h during ODS of light cycle oil (LCO) in batch and fixed bed reactors. The performance of the catalysts was discussed in terms of molybdenum oxide dispersion measured by oxygen chemisorption and acidity of the support.

Zhou et al. [2009] conducted experiments on direct oxidation of dibenzothiophene (DBT) based on molecular oxygen and iron tetranitrophthalocyanine (FePc(NO<sub>2</sub>)<sub>4</sub>) catalyst in hydrocarbon solvent under water-free condition for deep desulfurization. Conversion of DBT in decalin reached 98.7 wt.% at 100 °C and 0.3 MPa of initial pressure with 1 wt.% of FePc(NO<sub>2</sub>)<sub>4</sub> over the whole solution for 2 h. In addition to FePc(NO<sub>2</sub>)<sub>4</sub>, another two catalysts,



FePc(NO<sub>2</sub>)<sub>3</sub>NH<sub>2</sub> and FePc(NH<sub>2</sub>)<sub>4</sub>, were synthesized to investigate the effect of substituents of iron phthalocyanines on their catalytic activities. The results show that the catalytic activity of these phthalocyanines decreases in the order of FePc(NO<sub>2</sub>)<sub>4</sub> > FePc(NO<sub>2</sub>)<sub>3</sub>NH<sub>2</sub> > FePc(NH<sub>2</sub>)<sub>4</sub>, indicating that the electron-donating group has negative effect on the catalytic properties. Activity of FePc(NO<sub>2</sub>)<sub>4</sub> was kept unchanged after 5 runs of oxidation; whereas, activity of FePc(NH<sub>2</sub>)<sub>4</sub> decreased because of its decomposition. Oxidative desulfurization of a model fuel, 500 µg/g solution of DBT in decalin, was performed based on the catalytic oxidation using molecular oxygen and FePc(NO<sub>2</sub>)<sub>4</sub> catalyst. The lowest sulfur content in the model fuel could be decreased to less than 4 µg/g after the treatment of this oxidation and a combined adsorption.

Mesoporous HPW/SiO<sub>2</sub> modified with Ag species was used as the catalyst for the oxidative desulfurization of both model and real diesel oils. Yan et al. [2009] prepared three model diesel oils by using petroleum ether, benzene, and octene, respectively, as solvent and with dibenzothiophene (DBT) as the objective sulfur compound. The catalyst with a molar ratio of Ag to HPW being 2 (Ag<sub>2</sub>-HPW/SiO<sub>2</sub>) exhibits the highest catalytic activity; however, the catalytic activity decreases with further increase in Ag content. The results of nitrogen adsorption-desorption, X-ray diffraction, UV-vis, and energy dispersive spectroscopy show that isolated Ag<sup>+</sup> ion is located on the modified catalyst. The modification of HPW/SiO<sub>2</sub> with Ag species may combine the selective absorption capacity of Ag<sup>+</sup> for sulfur compounds with the catalytic activity of HPW, which is helpful to enhance the selective oxidative desulfurization. During the desulfurization process, the sulfur compounds were first selectively adsorbed on the catalyst surface by  $\pi$  complexation between Ag<sup>+</sup> and sulfur compounds, which could increase the probability of collision between sulfur compounds and catalytic active sites and then accelerate the oxidation reaction. The sulfur content in the real diesel oil reduced to 228 × 10<sup>-6</sup> from the original 1800 × 10<sup>-6</sup> over Ag<sub>2</sub>-HPW/SiO<sub>2</sub>; the desulfurization amount is 4.6% higher than that over the unmodified HPW/SiO<sub>2</sub>. In addition, the Ag-modified catalyst shows excellent reusability; after three reaction cycles, the desulfurization ratio of Ag<sub>2</sub>-HPW/SiO<sub>2</sub> is only slightly lower than that of the fresh catalyst.

Oxidation of thiophene and its derivatives was studied by Laszlo et al. [2008] using hydrogen peroxide (H<sub>2</sub>O<sub>2</sub>), t-butyl-hydroperoxide and Ti-Beta redox molecular sieve as selective oxidation catalysts. A new reaction pathway was discovered and investigated using C-13 NMR,

GC, GC-MS, HPLC, ion chromatography, and XANES. The thiophene oxidized to thiophene-sesquioxide [3a,4,7,7a-tetrahydro-4,7-epithiobenzo[b]-thiophene 1,1.8- trioxide] and the sesquioxide oxidized mostly to sulfate. 2-Methyl-thiophene and 2,5-dimethylthiophene also oxidized to sulfate and sulfone products. The Benzothiophene oxidation product was sulfone. This proposed new reaction pathway is different from prior literature, which reported the formation of thiophene 1,1-dioxide (sulfone ) as a stable oxidation product.

Asghar et al. [2009] conducted experiments on the oxidative desulfurization of model sulfur compounds such as dibenzothiophene and benzothiophene in toluene as a simulated light fuel oil with a mixture of hydrogen peroxide as the oxidant and various acids as the catalyst. The influences of various parameters including reaction temperature (T), acid to sulfur molar ratio (Acid/S), oxidant to sulfur molar ratio (O/S), type of acid, and the presence of sodium tungstate and commercial activated carbon as a co-catalyst on the fractional conversion of the model sulfur compounds were investigated. The experimental data obtained were used to determine the reaction rate constant of the model sulfur compounds and the corresponding activation energy. Moreover, the adsorption of model sulfur compounds on the commercial activated carbons was studied and the effects of different parameters such as temperature, and various chemical treatments on the adsorption of the sulfur compounds were investigated. Furthermore, the oxidative desulfurization of untreated kerosene with the total sulfur content of 1700 mg/lw was successfully investigated. These experiments were performed using formic acid as the catalyst and hydrogen peroxide as the oxidant at the mild operating conditions of  $T=50\text{ }^{\circ}\text{C}$ ,  $O/S=5$ , and the  $\text{Acid}/S=10$ . It was realized that about 87% of the total sulfur content of untreated kerosene could be removed after 30 min oxidation followed by liquid–liquid extraction.

Jianghua et al. [2009] prepared phosphomolybdic acid (HPMo) catalyst by modifying with tetramethyl ammonium chloride (TMAC), dodecyl trimethyl ammonium chloride (DTAC) and hexadecyl trimethyl ammonium chloride (HTAC) as the catalysts were prepared and characterized by FT-IR, XRD and SEM. The catalysts were evaluated for the oxidative desulfurization of benzothiophene (BT), dibenzothiophene (DBT) and straight-run diesel using hydrogen peroxide as an oxidant. Hexadecyl chains are more favorable to wrap up DBT to the catalytic center and form stable emulsion system with higher conversion rates of DBT. The shorter dodecyl chains can wrap up BT more suitably and bring smaller steric hindrance, which

display higher conversion rates of BT. The oxidative reactions fit apparent first-order kinetics, and the apparent activation energies of DBT are much lower than those of BT. The desulfurization rate of straight-run diesel can be up to 84.4% with the recovery rate of 98.1% catalyzed by [HPMo][HTAC]<sub>2</sub> in 2 h. When increasing the extraction times, the desulfurization rates increase, but the recovery rates of diesel decrease significantly.

### 2.3 BIODESULFURIZATION (BDS):

Another approach to produce ultra-low fuels is biodesulfurization (BDS) which can selectively remove sulfur from DBTs. BDS has the potential benefits of lower operation cost and production of valuable by products [Bagreev et al., 2005]. Sulfur compounds can be converted into hydroxyl biphenyl and its derivatives. BDS can be considered either an alternative or a complementary method to the conventional oil refining technology. Some of the isolated micro organisms capable of sulfur removal are not effective in commercial uses. Therefore, there is still a need to increase the rate of sulfur removal that may efficiently biodesulfurize the diesel.

#### 2.3.1 Recent studies in BDS

Li et al. [2005] isolated a new bacterial strain capable of selectively desulfurizing dibenzothiophene (DBT) from sludge. This organism, designated ZD-M2, clustered most closely with members of the genus *Microbacterium*, as determined by 16S rRNA gene sequence analysis. Metabolites produced by DBT desulfurization were identified by GC-MS, and two sulfur-free products, 2-methoxybiphenyl (2-MBP) and biphenyl, were detected in addition to 2-hydroxybiphenyl (2-HBP). This strain can also totally degrade 4,6-dimethyl-DBT, thiophene, benzothiophene and 70% diphenylsulfide.

Hou et al. [2005] successfully isolated Immobilization of the bacterium *Pseudomonas stutzeri* UP-1 from soil and sewage in the Shengli Oil field. Biodesulfurization (BDS) of dibenzothiophene (DBT) was carried out using immobilized *P. stutzeri* UP-1 (CGMCC No. 0974) in model system. The results show that sodium alginate (SA) is an appropriate material of immobilization. The optimized operation immobilization condition was 4 °C; the concentration of SA was 3% (w/v); and the ratio of SA (ml) to cells (g) was 20. The stability and life-time of immobilized cells were much better than those of the non-immobilized cells. The life-time of immobilized cells could reach 600 h by reactivation.

Caro et al. [2007] studied Biodesulfurization (BDS) process yields both in aqueous and biphasic media, with hexadecane as model oil. All batch assays were carried out at Erlenmeyer flasks scale, under different experimental conditions such as oil fraction phase percentages, substrate concentrations and cellular densities, using resting cell as operation mode. Providing that cell densities were not too high, both biocatalysts achieved better DBT conversion with higher biomass concentrations and lower oil fractions and DBT concentrations. Comparing aqueous and biphasic media it has been also proved that *P. putida* CECT 5279 strain was more sensitive for DBT mass transfer limitation, determining the preferable use in biphasic systems of IGTS8 to practical BDS process as well. Furthermore, the experimental results suggested there could be inhibitions effects by product accumulation in aqueous media, but these effects were not so clear in biphasic condition, because 2-hydroxybiphenyl (HBP) oil–water partition coefficient is very high.

Olmo et al. [2007] studied the production of a biocatalyst of *Rhodococcus erythropolis* IGTS8 able to desulfurize dibenzothiophene (DBT). Biomass growth rate and the development of removing sulfur capability during microorganism growth have been measured and modeled. Different growth media have been employed, different carbon (glucose, glutamic acid and citrate), nitrogen (ammonium and/or glutamic acid) and sulfur (DBT), dimethylsulfoxide (DMSO) and magnesium sulphate-sources have been used, as well as different DMSO concentrations (1300, 500, 250 and 50  $\mu\text{M}$ ), in order to study its influence on growth rate and desulfurizing capability. Experimental results show clear differences both in growth and in the biodesulfurization capability developed by cells depending on the media composition. To quantify the desulfurization capability a parameter has been defined: *DBDS*, biodesulfurization degree developed during growth, useful not only to compare the results achieved under different media and conditions but also to compare different microorganisms with desulfurization capability. Inside the experimental range studied, the best production media is composed of 20 g/l glucose, using 670 mg/l.  $\text{NH}_4^+$  and 1300  $\mu\text{M}$  DMSO as carbon, nitrogen and sulfur sources. A non-structured kinetic model to describe growth and desulfurizing capability development is proposed and applied by non-linear simple response fitting to all the experiments carried out. The model is able to describe all the experimental data with good statistical parameters.

Yang et al. [2007] designed an aqueous–organic two-layer partitioning and continuous process to make efficient use of growing cells for the biodesulfurization of diesel oils. This biphasic system was shown to have a significant advantage over batch and fed-batch processes in the maintenance of the biodesulfurization activity for an extended period of time. Specifically, it was demonstrated that in a 2-L bioreactor 1500 mg/l total sulfur was removed from 250 ml diesel oil within a 5-day period.

Mohebbali et al. [2007] reported the ability of a newly isolated bacterium, *Gordonia alkanivorans* RIPI90A to desulfurize both DBT and DBT-containing hexadecane during both the growth and resting stages, with conversion of DBT to 2-hydroxybiphenyl (2-HBP) via the 4S pathway. The highest specific activity, in terms of DBT-utilization occurred in cells harvested from the late exponential growth phase; the reaction rate and the specific activity were 182  $\mu\text{Mh}^{-1}$  and 56.34  $\mu\text{M 2-HBP g}^{-1}_{\text{dry cell weight h}^{-1}}$ , respectively. Suitable cell surface hydrophobicity allowed the cells to obtain the sulfur compounds directly from the organic phase. The main goal of this effort was to study the desulfurizing resting cells function in biphasic organic media and to provide information to maximize biocatalyst activity in the media. The optimal conditions for the desulfurization of DBT-containing hexadecane in a biphasic system including resting cell suspension (water/oil, 50: 50) were determined as 20 and 7 for cell concentration ( $\text{OD}_{660}$ ) and pH, respectively. The results suggest that this strain is of potential for the biodesulfurization of diesel oils.

Shavandi et al. [2009] cloned and sequenced the dszABC genes from newly reported dibenzothiophene biodesulfurizing bacterium, *Gordonia alkanivorans* RIPI90A. The overall nucleotide sequence similarity between the dszABC genes of *G. alkanivorans* RIPI90A and those of *Rhodococcus erythropolis* IGTS8 and *Gordonia nitida* were 83.1% and 83.2%, respectively. A gene transfer system for *G. alkanivorans* RIPI90A was established employing the *Escherichia coli*–*Rhodococcus* shuttle vector pRSG43 as suitable cloning vector, resulting in transformation efficiencies up to  $1.6 \times 10^{-5}$  CFUs  $\mu\text{g}^{-1}$  plasmid DNA. This stable vector was applied to cloning and efficient expression of the dsz genes under the control of lac promoter. The recombinant strain was able to desulfurize dibenzothiophene in the presence of inorganic sulfate and sulfur-containing amino acids. The maximum desulfurization activity by recombinant resting cells was increased 2.67-fold in comparison to the highest desulfurization activity of native resting cells.

Dehaghani et al. [2010] isolated a new dibenzothiophene (DBT) desulfurizing bacterium was from oil-contaminated soils in Iran. HPLC analysis and PCR-based detection of the presence of the DBT desulfurization genes (*dszA*, *dszB* and *dszC*) indicate that this strain converts DBT to 2-hydroxybiphenyl (2-HBP) via the 4S pathway. The strain, identified as *Rhodococcus erythropolis* SHT87, can utilize DBT, dibenzothiophene sulfone, thiophene, 2-methylthiophene and dimethylsulfoxide as a sole sulfur source for growth at 30 °C. The maximum specific desulfurization activity of strain SHT87 resting cells in aqueous and biphasic organic–aqueous systems at 30 °C was determined to be 0.36 and 0.47 l mol 2-HBP min<sup>-1</sup> (g dry cell)<sup>-1</sup>, respectively. Three mM DBT was completely metabolized by SHT87 resting cells in the aqueous and biphasic systems within 10 h. The rate and the extent of the desulfurization reaction by strain SHT87 suggest that this strain can be used for the biodesulfurization of diesel oils.

Bhatia et al. [2010] carried out the isolation of a DBT desulfurizing mesophilic bacterium, characterized as *Pantoea agglomerans* D23W3, from contaminated soils collected from refinery has been reported. HPLC analysis revealed that *P. agglomerans* D23W3 could convert DBT to 2-hydroxybiphenyl (2-HBP) via the 4S pathway and that it could degrade 93% of the 100mg/l DBT within 24 h of culture. In addition *P. agglomerans* D23W3 could also desulfurize 4,6-dimethyl DBT and benzothiophene which are among the most difficult DBT derivatives to be removed by HDS. Further, adapted cells of *P. agglomerans* D23W3 were found to remove 26.38–71.42% of sulfur from different petroleum oils with highest sulfur removal from light crude oil. Therefore, these researchers reported that *P. agglomerans* D23W3 has a potential for the BDS of the petroleum oils.

## **2.4 ADSORPTIVE DESULFURIZATION**

### **2.4.1 Recent studies in adsorptive desulfurization**

Tang et al. [2008] performed desulfurization of various model fuels containing about 500 µg/g sulfur were studied over the synthesized Y zeolite ([Ga]AlY) with a liquid hourly space velocity of 7.2 h<sup>-1</sup> at ambient conditions. The sulfur adsorption capacity was 7.0, 14.5, and 17.4 mg(S)/g adsorbent for thiophene, 4,6- dimethyldibenzothiophene (4,6-DMDBT), and tetrahydrothiophene (THT), respectively. The charges on S atom in thiophene, 4,6-DMDBT and THT, calculated by using density functional theory (DFT), are -0.159, -0.214 and -0.298,

respectively, implying that the S–M bond between the adsorption sites and thiophene is much weaker than that between the adsorption sites and THT or 4,6-DMDBT.

Li et al. [2009] conducted experiments for the deep desulfurization of diesel, a novel adsorption–bioregeneration system was constructed by combining adsorption and biodesulfurization processes. The sequence of adsorption capacity of DBT (dibenzothiophene) is AC (activated carbon) > NiY > AgY > alumina > 13X. The sequence of selectivity of DBT toward naphthalene is NiY > AgY > alumina ≈ 13X > AC. For hydrotreated diesel, MAS (mesoporous aluminosilicates) showed high adsorption capacity, while MCM-41 and NaY showed low adsorption capacity. The bioregeneration process of these adsorbents was also carried out with *P. delafieldii* R-8 cells. Adding *P. delafieldii* R-8 cells can improve DBT desorption from adsorbents. The desorption of DBT from adsorbents by bioregeneration follows the sequence: 13X > alumina > AgY > NiY > AC. Ag-MAS can be completely regenerated in *in situ* adsorption–bioregeneration system.

Meng et al. [2010] studied the desulfurization of model gasoline containing 600 mg/lw thiophene or dibenzothiophene (DBT) by selective adsorption over Ag<sup>+</sup> exchanged mesoporous material Al-MSU-S in a fixed adsorbent bed at ambient temperature and pressure. The results showed that the sulfur capacity increased with Al content incorporated in the silicate framework and Ag<sup>+</sup> exchange can effectively improve the desulfurization performance. The best adsorbent, Ag<sup>+</sup>/20%Al-MSU-S, has adsorption capacity of 5 or 20 ml model gasoline containing thiophene or DBT per gram adsorbent, respectively, before the detection limit in our experiments, as a result of  $\pi$ -complexation. The adsorbent can be regenerated more than six times by simple calcination in air at 350 °C without obvious losing the sulfur adsorption capacity.

Baeza et al. [2008] studied copper supported on zirconia used to separate low thiophene concentration from a mixture of 2000 mg/lw of thiophene in noctane at room temperature and atmospheric pressure. The results show that the capacity of copper on zirconia to adsorb thiophene increases as the copper content increases, reaching a maximum at a concentration of 3% of copper. The adsorption capacity also depends on the treatment used, and the higher capacities are observed in adsorbents treated with a flow of N<sub>2</sub>O at 90 °C. These samples possess notable saturation adsorption capacities of 0.49 mmol of thiophene per grams of adsorbent.

Mikhail et al. [2002] conducted experiments to find an economically attractive alternative method for desulfurization of petroleum fraction and to select a suitable adsorbing material. The solid materials; acid-activated kaolinite, acid-activated bentonite, charcoal, petroleum coke and cement kiln dust are selected to verify this purpose. Dimethyl disulfide compound has been used as a sulfur model compound to evaluate the adsorption efficiency of these solid materials. The acid-activated bentonite was found to be the most suitable adsorbent studied, at the lowest reaction temperature 30 °C. The higher efficiency of the activated-clay towards sulfur adsorption may be attributed to that, the silicate–silicate bentonite structure possesses Bronsted acid sites, which resulted from the dissociation of the water molecule in between silicate sheets. In addition, the clay surface, after acid treatment would possess positive hydrogen sites. Therefore, the increase in acid sites, disturbs the charge equilibrium in the bentonite-clay lattice, creates strain that arises new active sites for adsorption, which would interact more favorably with the basic sulfur compounds.

Wang et al. [2009] studied the effects of olefin on adsorptive deep desulfurization of gasoline over Ce(IV)Y zeolites via a FT-IR spectrometry and a fixed-bed adsorption technique at room temperature and atmosphere pressure by using model fuels containing thiophene and 1-octene as model compounds. The adsorptive selectivity for thiophene decreases significantly as the concentration of 1-octene increases. The difference in the FT-IR spectra between the Ce(IV)Y zeolite samples adsorbing the model fuels with and without 1-octene can be attributed to the stronger adsorption interactions of 1-octene with the Ce(IV)Y zeolite than those for thiophene. For minor content (500 µg/g) of thiophene and 1-octene, the FT-IR spectra show that the Ce(IV)Y zeolites have the preference to adsorb thiophene rather than 1-octene. However with the content of 1-octene increasing in the model fuel up to 150 mg/g, 1-octene can be adsorbed on the Ce(IV)Y zeolites remarkably, resulting in a descending adsorptive selectivity of the Ce(IV)Y for removing thiophene from the model fuel.

Since the conventional hydrodesulfurization process employed in the refinery industry is not suitable for mobile fuel cell applications (e.g. auxiliary power units, APUs), Wang et al. [2009] aimed at developing an alternative process and determining its technical feasibility. A large number of processes were assessed with respect to their application in fuel cell APUs. The



results revealed that a two-step process combining pervaporation and adsorption is a suitable process for the on-board desulfurization of jet fuel. Therefore, a pervaporation process with subsequent adsorption was selected for detailed investigation. Six different membrane materials and ten sorbent materials were screened to choose the most suitable candidates. Further laboratory experiments were conducted to optimize the operating conditions and to collect data for a pilot plant design. Different jet fuel qualities with up to 1675 mg/lw of sulfur can be desulfurized to a level of 10 mg/lw. The aim of developing a suitable process for the desulfurization of jet fuel in fuel cell APUs was thus achieved.

Muzic et al. [2010] studied removal of sulfur from diesel fuel by adsorption on a commercial activated carbon and 13X type zeolite in a batch adsorber. Kinetic characterization of the adsorption process was performed applying Lagergren's pseudo-first order, pseudo-second order and intraparticle diffusion models using data collected during experiments carried out to determine the sulfur adsorption dependency on time. The experiments investigating adsorption efficiency regarding initial sulfur concentration were also performed and the results were fitted to Langmuir and Freundlich isotherms, respectively. Activated carbon Norit SXRO PLUS was found to have much better adsorption characteristics. The process of sulfur adsorption on the fore mentioned activated carbon was further studied by statistically analyzing data collected during experiments which were carried out according to three-factor two-level factorial design. Statistical analysis involved the calculation of effects of individual parameters and their interactions on sulfur adsorption and the development of statistical models of the process.

Sano et al. [2005] proved that regeneration of used activated carbon fiber (ACF) with a conventional solvent was very effective in restoring its adsorption capacity. An integrated adsorption process for deep desulfurization of diesel fuel was proposed and examined. Conventionally hydrodesulfurized straight run gas oil (HDS-SRGO) having less than 50 mg/l sulfur was also adsorptively treated with ACF to attain the ultra low sulfur gas oil having less than 10 mg/l sulfur. The ACF, used in cleaning-up HDS-SRGO, was successively examined in straight run gas oil (SRGO) treatment to enhance its hydrodesulfurization (HDS) reactivity over conventional CoMo catalyst by removing the nitrogen and refractory sulfur species contained in

SRGO. Such integrated adsorption–reaction process makes it possible to utilize the maximum adsorption capacity of ACF and achieve ultra deep desulfurization of SRGO.

Selvavathi et al. [2009] conducted experiments on Adsorptive desulfurization (ADS) process for the refractory sulfur compounds viz., dibenzothiophene (DBT), 4-methylbenzothiophene (4MDBT) and 4,6-dimethyl-dibenzothiophene (4,6-DMDBT) present in diesel fuel (Gas oil). Two commercially available activated carbons A and B and modified forms of the same by HNO<sub>3</sub> treatment and Ni supported systems were used for the adsorption studies. The modified activated carbon samples A and B showed better adsorption capacity when compared with that of as received activated carbon samples and metal supported systems.

### ***How Adsorptive distillation came into picture?***

Various desulfurization techniques like hydrodesulfurization (HDS), oxidative desulfurization (ODS), bio-desulfurization (BDS) and adsorptive desulfurization are being investigated world over to produce ultra clean fuels. HDS is the most commonly used method of sulfur reduction of fossil fuels in refineries. Typically, it involves catalytic treatment with hydrogen to convert the various sulfur compounds to hydrogen sulfide. However, it requires the application of severe operating conditions and the use of especially activated catalysts for the production of fuels with very low levels of sulfur compounds. HDS is limited in treating benzothiophenes (BTs) and dibenzothiophenes (DBTs), especially DBTs having alkyl substituent on 4 and/or 6 positions. Moreover, the HDS process has reached a stage where increasing temperature and pressure is just not enough to remove last traces of sulfur without affecting the octane number.

In the oxidation process, the sulfur containing compounds is oxidized to sulfone by chemical reaction using various types of oxidants namely H<sub>2</sub>O<sub>2</sub>, H<sub>2</sub>SO<sub>4</sub>, etc. The sulfone compound is then easily extracted from the fuel because of its higher polarity. Reaction selectivity, safety and cost are important concerns for the selection of oxidants, catalysts and operating conditions in ODS processing. The catalytic systems reported in literature are mostly toxic and expensive.

Bio-desulfurization has drawn wide attention over the past decade. Considerable research has been done to extend the understanding of the enzymology and molecular genetics of the BDS system and to apply that into the design of the BDS bioreactor and bioprocesses.

In the adsorption process as an alternative processor complementary stage for the HDS process, the untreated refractory sulfur compounds can be selectively removed by an adsorbent at low temperatures and at ambient pressure. In addition, this method is more attractive because it is a low-energy demand process and that the various types of adsorbents are available. For example, various types of adsorbents including carbon aerogels, zeolites (Cu (I)-Y, Na-Y, etc.), activated carbon, organic waste derived carbons etc., have been examined. In addition, developed activated carbons such as PdCl<sub>2</sub>/AC or metal-loaded polystyrene based activated carbons have been used for the selective adsorption of thiophenic compounds.

In the adsorptive desulfurization technique, the active adsorbent is placed on a porous, non-reactive substrate that allows high surface area for the adsorption of sulfur compounds. Adsorption occurs when the sulfur molecules attach to the adsorbent and remain there separate from the fuel. Various investigators have utilized this technique for the removal of sulfur from various types of fuels and model oils by various types of adsorbents. Desulfurization by adsorption faces the challenge of developing easily remunerable adsorbent with a high adsorption capacity. Adsorbents developed must have high selectivity for the adsorption of refractory aromatic sulfur compounds that do not get removed during the HDS process.

## **2.5 IN-SITU PROCESS:**

In-situ coupling of adsorptive desulfurization and biodesulfurization is a new desulfurization technology for fossil oil. It has the merits of high-selectivity of biodesulfurization and high-rate of adsorptive desulfurization. It is carried out by assembling nano-adsorbents onto surfaces of microbial cells. In this work, In-situ coupling desulfurization technology of widely used desulfurization adsorbents of  $\gamma$ -Al<sub>2</sub>O<sub>3</sub>, Na-Y molecular sieves, and active carbon with *Pseudomonas delafieldii* R-8 were studied. Results show that Na-Y molecular sieves restrain the activity of R-8 cells and active carbon cannot desorb the substrate dibenzothiophene (DBT). Thus, they are not applicable to in-situ coupling desulfurization technology. Gamma-Al<sub>2</sub>O<sub>3</sub> can adsorb DBT from oil phase quickly, and then desorb it and transfer it to R-8 cells for

biodegradation, thus increasing desulfurization rate. It is also found that nano-sized  $\gamma\text{-Al}_2\text{O}_3$  increases desulfurization rate more than regular-sized  $\gamma\text{-Al}_2\text{O}_3$ . Therefore, nano-  $\gamma\text{-Al}_2\text{O}_3$  is regarded as the better adsorbent for this in-situ coupling desulfurization technology [Dehkordi et al., 2009].

Table 2.1 Removal summary of sulfur by HDS at optimized conditions

Process	Sulfur Compound	Fuel	Catalyst	System	S Conc. C <sub>0</sub> (mg/l)	Optimum Condition		% S Removal	Reference
						Temp	Pressure		
HDS	Alkyl DBTs	Gas oil	NiMo sulphide on Al <sub>2</sub> O <sub>3</sub> -Si support	Packed Bed	11,780	340 °C	4.9 MPa	94 %	Kunisada et. al., 2004
Deep HDS	Alkyl DBTs	Light cycle oil	Co-Mo supported on MCM-41	Packed Bed	21,900	350 °C	4.5 MPa	57 %	Turang and Song, 2003
Lab scale HDS	Alkyl DBTs	Middle distillates	NiMo/ $\gamma$ -Al <sub>2</sub> O <sub>3</sub>	Trickle Bed	16,740	350 °C	4.0 MPa	90 %	Pedemera et. al., 2003
Lab Scale Deep HDS	Alkyl DBTs	Diesel	P and Ni-Al <sub>2</sub> O <sub>3</sub> supported Mo oxycarbides	-	520	340 °C	4.0 MPa	50 %	Costa et. al., 2005
HDS	Thiophene	n-Heptane	FeS-MoS supported on Al <sub>2</sub> O <sub>3</sub> and carbon	-	1000	280 °C	0.1 MPa	30 %	Hubaut et. al., 2006
Ultra Deep HDS	Alkyl DBTs	SRGO	Co-Mo/ Al <sub>2</sub> O <sub>3</sub>	Fixed Bed Microreactor	17,030	300 °C	5 MPa	99 %	Al-Barood and Stanislaus, 2007
HDS	DBT	Decahydronaphthalene	Ni-Mo(W) and Co-Mo(W) over Zr doped SiO	Fixed Bed	10,000	340 °C	3 Mpa	93 %	Rodriguez-Castelloin et. al., 2008
HDS	4,6-DMDBT	n-Heptane	Sulfided NiMoP/ Al <sub>2</sub> O <sub>3</sub> - zeolite	Fixed Bed Microreactor	450	340 °C	4.0 MPa	60 %	Richard et. al., 2009
HDS	Alkyl DBTs	Hexadecane	CoMo/SiO modified with Ti	Fixed Bed	3000	440 °C	5.5 MPa	60 %	Zepeda et. al., 2009
HDS	4,6-DMDBT	-	NiMo/Al-SBA-15	Batch	159	300 °C	7.3 MPa	80 %	Klimova et. al., 2010

Table 2.2 Removal summary of sulfur by ODS at optimized conditions.

Process	Sulfur Compound	Model Oil	Reagent	System	S Conc. $C_0$ (mg/l)	Optimum Conditions		% S Removal	Reference
						Temp	pressure		
Oxidation - Absorption	DBT	n-Octane	H <sub>2</sub> O <sub>2</sub> + Activated C	Batch	800	60 °C	1 atm	99%	Yu et. al., 2005
Oxidation - Absorption	DBT	Toluene (40%) Hexane (60 %)	H <sub>2</sub> O <sub>2</sub>	Batch	5000	50 °C	1 atm	92%	Ali et. al., 2006
Oxidation - Absorption	DBT	Iso -Octane	t-BuOOH + HPWA - SBA -15	Batch	174	70 °C	1 atm	97.43%	Yang et. al., 2007
Oxidation	BTs	Decalin		Batch	500	40 °C	1 atm	98%	Lu et. al., 2006
Ultrasound Oxidation	DBT	Toluene	H <sub>2</sub> O <sub>2</sub>	Batch	3000	75 °C	1 atm	98%	Mei et. al., 2009
Oxidation	Tetrahydrothiophene	Cyclohexane	H <sub>2</sub> SO <sub>4</sub>	Batch	2000	22 °C	1 atm	99%	Nehlsen J.P., 2009
Oxidation	Thiophene+ 3-Methylthiophene	n-Heptane	H <sub>2</sub> O <sub>2</sub> + Formic acid	Batch	500	50 °C	1 atm	80%	Lanju et. al., 2010
Oxidation	DBT+4,6-DMDBT	Octane	Na <sub>2</sub> WO <sub>4</sub> + 30% H <sub>2</sub> O <sub>2</sub> + CH <sub>3</sub> CO <sub>2</sub> H	Batch	500	70 °C	1 atm	100%	Al-Shahrani et al., 2007
Oxidation	DBTs	Hexadecane	H <sub>2</sub> O <sub>2</sub> + V <sub>2</sub> O <sub>5</sub> based catalysts	Batch	500	60 °C	1 atm	99%	Caero et al., 2008
Oxidation	Alkylated DBTs	Diesel	H <sub>2</sub> O <sub>2</sub> + Mo/ $\gamma$ -Al <sub>2</sub> O <sub>3</sub>	Batch	320	60 °C	1 atm	97%	Gutierrez et al., 2008

**Table 2.3 Removal summary of sulfur by adsorption at optimized conditions**

Process	Sulfur Compound	Model oil	Adsorbent	System	S Conc. C <sub>0</sub> (mg/l)	Optimum Conditions		% S Removal	Reference
						Temp	Pressure		
Adsorption	DBT	n-hexadecane	Carbon Aero-gels	Batch	50	25 °C	1 atm	90%	Haji S.*2005
Adsorption	DBT	Crude Oil	Intermetallic Powder	PACKED Bed	250	25 °C	1 atm	55%	Lu S.H. 2000
Adsorption	DBT	Toluene(45%) Hexane (55%)	Ruthenium Complexes	Batch	40	25 °C	1 atm	50%	Mckinley, 2003
Adsorption	4,6 Me <sub>2</sub> DBT	Toluene(45%) Hexane (55%)	Ruthenium Complexes	Batch	40	25 °C	1 atm	40%	Mckinley, 2003
2 step Adsorption	Thiopenes	Gas Oil	Activated Carbon	Packed Bed	300	70 °C	1.5 atm	88%	Sano et al, 2004
Adsorption	Thiopenes	Diesel	CuCl/γ-Al <sub>2</sub> O <sub>3</sub>	Fixed Bed	140	25 °C	1 atm	99%	Gongshin Q., 2006
Adsorption	DBT	-	Activated Carbon	Batch	178	25 °C	1 atm	95%	Ania et al, 2007
Adsorption	Thiophene + DBT	n- hexane	Zeolites from coal fly ash	Batch	500	30 °C	1 atm	63%	Ngamcharu ssrivichai et al, 2007
Adsorption	4,6-DMDBT	cyclohexane	NiMoP/ Al <sub>2</sub> O <sub>3</sub> catalyst +NaY zeolites	Fixed Bed	450	340 °C	40 atm	56%	Richard et al, 2007
Alkylation	3-methylthiophene	n-Heptane	Silica-supported 12-phosphotungstic zeolite	Slurry tank reactor	340	85 °C	1 atm	60%	Arias et al, 2008
Adsorption	4,6-	n-Nonane	Gallium+Y	Fixed Bed	500	60 °C	-	97%	Tang et al.,

	DMDBT		zeolite	flow reactor						2008
Bond cleavage	Thiopenes	n-Hexane	(C <sub>5</sub> Me <sub>5</sub> )Rh(PMe <sub>3</sub> )(Ph)H	Batch	-	64 °C	1 atm	-	-	Myers et al., 2009
Selective Adsorption	-	Commercial diesel	Metallic nickel nanoparticles supported on mesoporous silica	Fixed bed	11.7	200 °C	-	99%	-	Park et al, 2008
Adsorption	Thiopene	n-Octane	Copper supported on zirconia	Fixed bed	2000	180 °C	-	99%	-	Baeza et al, 2009
Ractive Adsorption	Thiopene		Ni/SiO <sub>2</sub> and Ni/ZnO	Fixed bed		300 °C	0.02			Bezverkhyy et al, 2010
Adsorption	DBT sulfone	-	Alumina	Packed column	700	200 °C	-	30%		Etemadi and Yen, 2010



Table 2.4 Removal summary of sulfur by adsorption at optimized conditions

Process	Sulfur Compound	Model oil	Microorganism	System	S Conc. C <sub>0</sub> (mg/l)	Optimum Conditions		% S Removal	Reference
						Temp	Pressure		
4S	DBT	n-Hexadecane	Bacterium, strain RIPI-22	Batch	100	30 °C	-	77%	Rashtchi et al, 2006
Biocatalytic oxidation	Organosulfides and THs	Straight run diesel fuel	Caldariomyces fumago	Batch	1600	25 °C	1atm	99%	Ayala et al, 1998
BDS	DBT +4,6-DMDBT	Light gas oil	Sphingomonas subarctica T7b	Fermenter	280	27 °C	-	94%	Gunam et al, 2006
4S	DBT	Tetradecane	<i>Mycobacterium goodii</i> X7B	Batch	200	40 °C	-	99%	Li et al, 2006
4S	DBT	n-tridecane	<i>Bacillus subtilis</i> WU-S2B	Batch	100	50 °C	-	50%	Kirimura et al, 2000
BDS	DBT	Ethanol	<i>Microbacterium</i> strain ZD-M2	Batch	36	30 °C	-	94%	Li et al, 2005
BDS	DBT	n-Hexadecane	<i>Pseudomonas stutzeri</i> UP-1	Batch	500	31 °C	-	74%	Hou et al, 2005
BDS	DBT	Decane	<i>Rhodococcus erythropolis</i> ATCC53968	Interface Bioreactor	184	30 °C	-	90%	Oda and Ohtaal, 2002
BDS	DBT	n-Hexadecane	<i>Rhodococcus</i> sp. strain P32C1	Batch	1000	30 °C	-	75%	Maghsoudi et al, 2001
BDS	-	Hydrodesulphurised diesel oil	<i>Pseudomonas dekafieldii</i> R-8	Fermenter	591	30 °C	-	47%	Guobbin et al, 2005
4S	DBT	Hexadecane	<i>Gordonia alkanivorans</i> RIPI90A	Batch	100	30 °C	-	90%	Mohebbi et al, 2006
4S	DBT	Hydrodesulphurised diesel oil	<i>Mycobacterium</i> sp. X7B	Batch	535	45 °C	-	86%	Li et al, 2009

4S	DBT	Hexadecane	<i>Rhodococcus erythropolis</i> IGTS8	Batch	100	30 °C	-	80%	Caro et al, 2009
4S	DBT	n-heptane	<i>Gordonia alkanivorans</i> strain 1B	Batch	100	35 °C	-	63%	Alves et al, 2009
BDS	DBT	n-tridecane	<i>Mycobacterium phlei</i> WU-F1	Batch	150	50 °C	-	99%	Furuya et al, 2001
Two layer continuous process	DBT	Hexadecane	<i>Rhodococcus globerulus</i> DAQ3	Fed Batch	1500	30 °C	-	20%	Yang et al, 2007
4S	DBT	Tetradecane	<i>Mycobacterium goodii</i> X7B	Fed Batch	200	40 °C	-	99%	Li et al, 2010
4S	DBT +4,6-DMDBT	-	<i>Mycobacterium</i> sp-ZD-19	Batch	92	30 °C	-	100%	Chen et al, 2010

**3.1 GENERAL**

In the present study, commercial activated carbon (CAC) and alum impregnated activated carbon (AICAC) have been explored for the removal of sulfur from model oil (Dibenzothiophene (DBT) dissolved in iso-octane). Experimental details of the study have been presented in this chapter. These details include characterization of adsorbents, batch adsorption studies and optimization of experimental parameters.

**3.2 CHARACTERIZATION OF ADSORBENTS**

CAC was supplied by Zeo-Tech adsorbents Pvt. Ltd, New Delhi, India. CAC in the particle range of 0.5 to 1 mm were only used in the present study. The physico-chemical characteristics of CAC and AICAC were determined using standard procedures as discussed below:

**3.2.1 X-Ray diffraction (XRD) analysis**

The XRD analysis was done using Cu-K $\alpha$  as a source and Ni as a filter media, and K radiation maintained at 1.542 Å. Goniometer speed was kept at 2° min<sup>-1</sup>. The range of scanning angle (2 $\theta$ ) was kept at 10-90°. The intensity peaks indicate the values of 2 $\theta$ , where Bragg's law is applicable. The identification of compounds was done using the ICDD library.

**3.2.2 Scanning electron microscope (SEM) and energy dispersive x-ray (EDX) study**

To understand the morphology of the adsorbents before and after the adsorption of DBT, and to study the chemical composition and the distribution of the elements in the adsorbents, a SEM QUANTA, Model 200 FEG, USA was used. The samples were first gold coated using Sputter Coater, Edwards S150, which provides conductivity to the samples, and then the SEMs and EDX spectra were taken.

**3.2.3 Fourier transform infrared (FTIR) spectroscopy**

FTIR spectrometer (Thermo Nicolet, Model Magna 760) was employed to determine the presence of functional groups in adsorbents before and after the adsorption of DBT at room temperature. Pellet (pressed-disk) technique was used for this purpose. The spectral range chosen

For statistical calculations, the levels for the four main variables  $X_1$  ( $X_1(C_0)$ ),  $X_2$  (m),  $X_3$  (t),  $X_4$  (T)) were coded as  $x_i$  according to the following relationship

$$x_i = (X_i - X_0) / \delta X \quad (1)$$

Where  $x_i$  is coded (dimensionless) value of  $X_i$ ,  $X_0$  is value of the  $X_i$  at the centre point and  $\delta X$  presents the step change. For second level of variable  $X_2$  (m=7 mg/l), the coded (dimensionless) value is calculated as follows:

$$x_i = [(X_i - X_0) / \delta X] = [(2 - 7) / 5] = -1 \quad (2)$$

where,  $X_0$  (=7) is value of the  $X_i$  (= m) at the centre point,  $\delta X$  = 5 for  $X_2$  (m).  $\delta X$  is constant difference between any two levels of m. The equally spaced value of  $x_i$  are designated as -2, -1, 0, +1 and +2 are given in Table 4.2.

A second-order polynomial model with interaction terms was fitted to experimental data obtained from experimental runs conducted. This model is given by following equation:

$$Y = b_0 + \sum b_i X_i + \sum b_{ii} X_i^2 + \sum b_{ij} X_i X_j \quad (3)$$

where,  $Y$  is the percentage DBT removal,  $b_0$  is the offset term,  $b_i$  is the first order term,  $b_{ii}$  is the second order main effect, and  $b_{ij}$  is the interaction effect.

### 3.5 EXPERIMENTAL PROCEDURE

For each experimental run, 50 ml solution of known concentration of sulfur in iso-octane was taken in 100 ml conical flask containing pre-weighted amount of CAC. These flasks are agitated at constant shaking rate of 150 rpm in a temperature controlled orbital shaker (Remi Instruments, Mumbai) maintained at 10-50 °C for the experiments carried out. The Samples were withdrawn at appropriate time intervals. Due to the particles suspension, all the samples were centrifuged (Research Centrifuge, Remi scientific works, Mumbai) at 10,000 rpm for 5 min and the supernatant liquid was analyzed for residual concentration of DBT.

For adsorption isotherms, sulfur solution of different concentrations ( $C_0 = 50 - 1000$  mg/l) were agitated with optimum dose of adsorbent till the equilibrium was achieved. The effect of temperature on the sorption characteristics was investigated by determining the adsorption isotherms at 288, 303 and 318 K. The residual sulfur concentration of the solution was then determined.

The percentage removal of sulfur and the equilibrium adsorption uptake in solid phase,  $q_e$  (mg/g), were calculated as follows:

$$\text{Percentage sulfur removal} = 100 \frac{(C_0 - C_e)}{C_0}$$

$$\text{Amount of adsorbed sulfur per gram solid, } q_e = \frac{(C_0 - C_e)}{m}$$

where  $C_0$  is the initial sulfur concentration (mg/l),  $C_e$  is the equilibrium sulfur concentration (mg/l), and  $m$  is the mass of the adsorbent (g).

#### 4.1 GENERAL

The meticulous discussion on the results of the experiments conducted for the removal of sulfur in the form of dibenzothiophene (DBT) by commercial activated carbon (CAC) and alum impregnated activated carbon (AICAC) is given in this chapter. These results include: characterisation of CAC and AICAC, central composite design (CCD) analysis, adsorption isotherm modeling, and adsorption thermodynamic study.

In this chapter, first all the discussion is given in the form of text. Tables and figures discussed in the text follow the text at the end of the chapter.

#### 4.2 CHARACTERIZATION OF ADSORBENTS

Morphological and structural characteristics, SEM, EDX and XRD analysis of blank and DBT loaded CAC and AICAC were carried out. The SEM of blank and DBT loaded CAC and AICAC are shown in Fig. 4.1. The figure reveals surface texture and porosity of the blank and DBT loaded adsorbents. It can be inferred from these figures that the surface texture of the blank adsorbents changes after the DBT adsorption.

Fig. 4.2(a) and 4.2(b) shows the EDX of CAC and AICAC before and after adsorption of DBT. Elemental compositions of blank and DBT loaded CAC and AICAC are given in Table 4.1(a) and 4.1 (b), respectively. Blank and DBT loaded CAC were found to be 11.08% and 11.40% oxygen; 81.87% and 77.18% carbon, respectively. In the same way blank and DBT loaded AICAC were found to be 9.09% and 14.4% oxygen; 83.87% and 69.47% carbon, respectively. In addition, DBT loaded CAC was found to contain 3.44% aluminum and 0.54% sulfur and DBT loaded AICAC was found to contain 2.89% aluminum and 0.4% of sulfur. Thus, sulfur is observed in DBT loaded CAC and AICAC. It is due to the loading of DBT on the adsorbents.

Fig 4.3 shows the XRD pattern of blank and DBT loaded CAC. XRD spectra of CAC shows the presence of Moganite ( $\text{SiO}_2$ ), Akdalaite  $[(\text{Al}_2\text{O}_3)_4 \cdot \text{H}_2\text{O}]$ , Tamarugite  $[\text{NaAl}(\text{SO}_4)_2 \cdot 6\text{H}_2\text{O}]$  and Fersilicate (FeSi) as major components. Peaks of DBT were observed in

DBT loaded CAC. The FTIR spectra of blank and DBT loaded CAC and AICAC were shown in Fig. 4.4(a) and 4.4(b). The FTIR analysis showed the appearance of some new groups in the spectra of DBT loaded CAC and AICAC. Transmittance around  $1100\text{ cm}^{-1}$  region is due to the vibration of  $-\text{CO}-$  group in lactones and  $-\text{COH}$  stretching and  $-\text{OH}$  deformation. The band around  $1400\text{ cm}^{-1}$  in CAC may be attributed to the carboxyl-carbonate structures. These characteristics indicate that  $-\text{CO}-$ ,  $-\text{OH}$  and  $-\text{COH}$  groups are effective in the adsorption of DBT onto CAC.

### 4.3 CCD ANALYSIS AND FITTING OF SECOND-ORDER POLYNOMIAL EQUATION (ANOVA)

A full central composite (CC) design (4 factor and 5 level) has been used in the present study as the experimental design model. Percentage DBT removal has been taken as a response of the system, while four process parameters, namely,  $C_0$ : 100-900 mg/l;  $m$ : 2-22 g/l;  $t$ : 15-735 min; and  $T$ : 10-50 °C, have been taken as input parameters. The variables and their levels are given in Table 4.2. The results of the  $Y$  (response) of DBT removal by adsorption were measured according to design matrix and the measured responses are listed in Table 4.3(a) and 4.3(b) for both adsorbents. Linear, interactive, quadratic and cubic models were fitted to the experimental data to obtain the regression equations. Two different tests namely sequential model sum of squares and model summary statistics were carried out in the present study to decide about the adequacy of various models. The results of these tests are given in Table 4.4(a) and 4.4(b). Cubic model was found to be aliased. Sequential model sum of squares showed that the  $p$  value was lower than 0.0001 for quadratic model (Table 4.4), therefore, this model could be used for further study. Quadratic model was found to have maximum “Adjusted R-Squared” and the “Predicted R-Squared” values. Therefore, quadratic model was chosen for further analysis.

An empirical relationship expressed by second-order polynomial equation was fitted between the response and the input variables. The final equations obtained in coded units are given below:

$$\text{PR} = 33.836 - 9.21562X_1 + 4.97433X_2 + 0.742106X_3 + 0.178647X_4 - 3.36222X_1^2 - 1.2639X_2^2 - 5.78717X_3^2 - 3.35073X_4^2 - 3.80009X_1*X_2 - 1.85176 X_1*X_3 + 3.793369 X_1*X_4 - 0.24876X_2*X_3 + 0.979581X_2*X_4 - 1.61923X_3*X_4 \quad (4.1)$$

$$PR = 33.836 - 9.68607X_1 + 5.202424X_2 + 1.014164X_3 - 0.09057X_4 - 2.87054X_1^2 - 1.26048X_2^2 - 5.7575X_3^2 - 3.13168X_4^2 - 3.97846X_1*X_2 - 2.05137X_1*X_3 + 4.196603X_1*X_4 + 0.275541X_2*X_3 + 0.966404X_2*X_4 - 1.58594X_3*X_4 \quad (4.2)$$

ANOVA is a statistical technique that subdivides the total variation in a set of data into component parts associated with specific sources of variation for the purpose of testing hypotheses on the parameters of the model. The statistical significance of the ratio of mean square variation due to regression and mean square residual error was tested using ANOVA. The ANOVA for the second-order equations are presented in Table 4.5(a) and 4.5(b). The ANOVA indicated that the equation adequately represented the actual relationship between the response (the percentage removal of DBT) and the significant variables. According to ANOVA (Table 4.5(a) and 4.5(b)), the Fisher  $F$  values for all regressions were higher. The large value of  $F$  indicates that most of the variation in the response can be explained by the regression equation. The associated  $p$  value is used to estimate whether  $F$  is large enough to indicate statistical significance.  $p$  values lower than 0.05 indicates that the model is statistically significant.

The ANOVA result for the DBT removal by CAC and AICAC shows  $F$  - value of 16.50796 and , which implies that the terms in the model have a significant effect on the response. The model gives coefficient of determination ( $R^2$ ) value of 0.9390 and an adjusted- $R^2$  value of 0.8821 for CAC, and 0.9369 and 0.8781 for AICAC, which is high and advocates a high correlation between the observed and the predicted values. The probability  $p$  ( $\sim 0.0001$ ) is less than 0.05. This indicates that the model terms are significant at 95% of probability level. Any factor or interaction of factors with  $p < 0.05$  is significant. The ANOVA table obtained from the response surface quadratic model shows that  $C_0$ ,  $m$ ,  $t^2$ ,  $T^2$ ,  $C_0^2$ ,  $C_0.m$  and  $C_0.T$  are significant. For AICAC,  $C_0$ ,  $m$ ,  $t^2$ ,  $T^2$ ,  $C_0.m$  and  $C_0.T$  were found to be significant. The constant, which does not depend on any factors and interaction of factors, shows that the average removal of DBT from model oil is 33.83% for both adsorbents respectively, and that this average removal is independent of the factors set in the experiment. The ANOVA analysis for CAC indicates a linear relationship between  $Y$  and with that of  $C_0$ ,  $m$  and  $t^2$ ; and the quadratic relationship with that of  $T^2$ ,  $C_0^2$ ; and the product of  $C_0$  with  $m$  and  $T$ . For AICAC,  $Y$  showed linear relation with  $C_0$ ,  $m$  and  $t^2$ ; and the quadratic relationship with that of  $T^2$ ,  $C_0.m$ ; and the product of  $C_0$  with  $m$



and  $T$ . The analysis shows that the form of the model chosen to explain the relationship between the factors and the response is correct. "Adeq Precision" measures the signal to noise ratio. A ratio greater than 4 is desirable. For the present study signal to noise ratio was found to be 13.751, which indicates adequate signal. Therefore, quadratic model can be used to navigate the design space.

Data were also analyzed to check the normality of the residuals. A normal probability plot or dot diagrams of these residuals are shown in Fig. 4.5(a) and 4.5(b). It is seen in Fig. 4.5(a) and fig. 4.5(b) that the developed model is adequate for both CAC and AICAC because the residuals for the prediction for most of the responses are less than 10% and the residuals tend to be close to the diagonal line. Fig. 4.6(a) and 4.6(b) shows the relationship between the actual and predicted values of  $Y$  for adsorption of DBT onto CAC and AICAC, respectively.

#### **4.4 EFFECT OF VARIOUS PARAMETERS ON DBT REMOVAL EFFICIENCY**

##### **4.4.1 Effect of adsorbent dosage ( $m$ ) and temperature ( $T$ )**

To study the effect of  $m$  on DBT removal, experiments were carried out by varying  $m$  from 5 to 22 g/l and under different  $T$  from 10 to 50 °C at  $C_o = 500$  mg/l. The results are plotted in Fig. 4.7(a) and Table 4.3(a). This figure clearly shows that at any fixed  $T$ , the removal of DBT was found to be increasing with an increase in the  $m$  from 5 g/l to 22 g/l. The removal remained unchanged for  $m > 20$  g/l for CAC. The increase in the adsorption with the CAC dosage can be attributed to the availability of greater surface area and more adsorption sites. At  $m < 20$  g/l, the CAC surface becomes saturated with DBT and the residual DBT concentration in the solution is large. With an increase in  $m$ , the DBT removal increases due to increased DBT uptake by the increased amount of CAC. For  $m > 20$  g/l, the incremental DBT removal became low. At about  $m = 20$  g/l, the removal efficiency became almost constant at for DBT removal by alumina.

At any particular  $m$ , DBT removal increased with an increase in  $T$  (Fig. 4.7(a)). Since adsorption is, generally, an exothermic process, it would be expected that an increase in  $T$  of the adsorbate-adsorbent system would result in decreased removal efficiency. The adsorption process is controlled by the diffusion process (intraparticle transport-pore diffusion), the removal efficiency showed an increase with an increase in temperatures up 30 °C and after this removal is

decreasing. This is basically due to the fact that the diffusion process is an endothermic process [Weber et al., 1972].

Similarly, the effect of  $m$  and  $T$  on removal DBT using AICAC carried out by varying  $m$  from 5 to 22 g/l and under different  $T$  from 10 to 50 °C at  $C_0 = 500$  mg/l can be deduced from Fig. 4.8(a).  $m$  affected the adsorption process in a similar fashion for reasons mentioned above but its affect was not as pronounced as in previous case.

#### 4.4.2 Effect of initial concentration ( $C_0$ ) and reaction time ( $t$ )

The effect of  $t$  and  $C_0$  on removal of DBT onto CAC under varying  $t$  (195-555 min) and  $C_0$  (100-700 mg/l) at  $m = 20$  mg/l and  $T = 30$  °C is plotted in Fig. 4.7(b). It is evident from the figure that at constant  $t$ , the DBT removal decreases with an increase in  $C_0$ , although when estimated in terms of the actual amount of DBT adsorbed per unit mass of adsorbent, it increased with an increase in  $C_0$ . The amount adsorbed increased with an increase in the adsorbate concentration due to the decrease in the resistance for the uptake of DBT from the solution. At constant  $C_0$ , conversion increased with an increase in time, reached maximum around 6 h, and thereafter remained constant.

In a similar way the effect of  $C_0$  and  $t$  on removal of DBT onto CAC under varying  $t$  (195-555 min) and  $C_0$  (100-700 mg/l) at  $m = 20$  mg/l and  $T = 30$  °C is plotted in Fig. 4.8(b). Negligible variation of response with  $C_0$  indicates the capacity of AICAC to handle much larger concentrations. For AICAC also, conversion increased with an increase in time at any  $C_0$ , reached maximum around 6 h, and thereafter remained constant.

#### 4.5 ADSORPTION EQUILIBRIUM STUDY

To optimize the design of an adsorption system for the adsorption of adsorbates, it is important to establish the most appropriate equilibrium correlation. Various isotherm equations such as the Freundlich, Langmuir, Redlich-Peterson (R-P), and Temkin equations, have been used to describe the equilibrium characteristics of adsorption. For low adsorbate loadings, Henry's law is valid. The Freundlich isotherm is derived by assuming a heterogeneous surface with a non-uniform distribution of heat of adsorption over the surface. Whereas, in the Langmuir theory, the basic assumption is that the sorption occurs at specific homogeneous sites within the

adsorbent. The Langmuir equation assumes monolayer sorption onto a surface with a finite number of identical sites, and it is given by

$$q_e = \frac{q_m K_L C_e}{1 + K_L C_e} \quad (4.3)$$

where,  $q_m$  is the monolayer adsorption capacity (mg/g) and is a constant, and  $K_L$  is a constant related to the free energy of adsorption ( $K_L = e^{-\Delta G/(RT)}$ ). It is the reciprocal of the concentration at which the adsorbent is half-saturated.  $C_e$  is the equilibrium liquid-phase concentration (given in units of mg/l). The Freundlich equation is given by

$$q_e = K_F C_e^{1/n} \quad (4.4)$$

Where,  $K_F$  is a constant that indicates the adsorption capacity of the adsorbent ( $\text{dm}^3/\text{g}$ ) and  $1/n$  is a constant that gives the intensity of adsorption. The R-P equation is written as

$$q_e = \frac{K_R C_e}{1 + a_R C_e^\beta} \quad (4.5)$$

where,  $K_R$  (given in units of l/g) and  $a_R$  (given in units of l/g) are the R-P isotherm constants and  $\beta$  is an exponent, the value of which lies between 0 and 1. For high concentrations, eq 4.5 reduces to the Freundlich isotherm with  $K_F = K_R/a_R$  (given in units of l/mg) and the heterogeneity factor given as  $1/n = 1 - \beta$ .

The Temkin isotherm is given as

$$q_e = B_T \ln(K_T C_e) \quad (4.6)$$

This isotherm contains a factor,  $K_T$  that explicitly takes into account the interactions between adsorbing species and the adsorbent.

Because of the inherent bias resulting from linearization, Marquardt's percent standard deviation (MPSD) function of nonlinear regression basin was used in this study to determine the best-fit isotherm model to represent the experimental equilibrium data.

The MPSD value is frequently used to test the adequacy and accuracy of the model fit with the experimental data. It is somewhat similar to the geometric mean error distribution, but is modified by incorporating the number of degrees of freedom.

The MPSD value is given by

$$MPSD = 100 \sqrt{\frac{1}{n-p} \sum_{i=1}^n \left( \frac{q_{e, \text{exp}} - q_{e, \text{calc}}}{q_{e, \text{exp}}} \right)^2} \quad (4.7)$$

The isotherm constants for the four isotherms studied, and the coefficient of determination,  $R^2$  with the experimental data are listed in Table 4.6. The  $R^2$  values for Redlich-Peterson are closer to unity in comparison to the values obtained for other isotherms, and also the MPSD error values are least for the fit of Redlich-Peterson. Therefore, Redlich-Peterson is the best-fit isotherm equation for the adsorption of DBT at all temperatures. Fig. 4.10 presents how well the Redlich-Peterson fits the data for DBT-CAC system at all temperatures.

#### 4.6 ESTIMATION OF THERMODYNAMIC PARAMETERS

The Gibbs free energy change of the adsorption process is related to the adsorption equilibrium constant by the classical Van't Hoff equation:

$$\Delta G^0_{ads} = -RT \ln K_{ads} \quad (4.8)$$

The Gibbs free energy change is also related to the change in entropy and the heat of adsorption at a constant temperature, as given by the equation

$$\Delta G^0 = \Delta H^0 - T\Delta S^0 \quad (4.9)$$

The previous two equations give the relation

$$\ln K_{ads} = \frac{-\Delta G^0_{ads}}{RT} = \frac{\Delta S^0}{R} - \frac{\Delta H^0}{R} \left( \frac{1}{T} \right) \quad (4.10)$$

where  $\Delta G^0_{\text{ads}}$  is the free energy change (expressed in units of kJ/mol),  $\Delta H^0$  the change in enthalpy (given in units of kJ/mol),  $\Delta S^0$  the entropy change (given in units of kJ/mol K),  $K_{\text{ads}}$  the equilibrium constant of interaction between the adsorbate and the CAC surface, T the absolute temperature (given in Kelvin), and R the universal gas constant (R) 8.314 J/mol K). Thus,  $\Delta H^0$  can be determined by the slope of the linear Van't Hoff plot, i.e., as  $\ln K_{\text{ads}}$  vs  $(1/T)$ , using the equation

$$\Delta H^0 = \left[ R \frac{d \ln K_D}{d(1/T)} \right] \quad (4.11)$$

The values of  $\Delta G^0$ ,  $\Delta H^0$  and  $\Delta S^0$  for DBT – CAC system is shown in Table 4.7.  $\Delta G^0$  values were negative indicating that the sorption process led to a decrease in Gibbs free energy and that the adsorption process is feasible and spontaneous. The adsorption of DBT onto CAC is endothermic in nature, giving a positive value of  $\Delta H^0$ . The adsorption process in the DBT–CAC–iso-octane system is a combination of two processes: (a) the desorption of the solvent (hexane) molecules previously adsorbed, and (b) the adsorption of the adsorbate species. The DBT molecules have to displace more than one hexane molecule for their adsorption, and this results in the endothermicity of the adsorption process. Therefore,  $\Delta H^0$  is positive. The positive value of  $\Delta S^0$  suggests increased randomness at the solid/solution interface with some structural changes in the adsorbate and the adsorbent and an affinity of the adsorbent towards DBT.

**TABLES**

**Table 4.1(a). Elemental composition of blank and DBT loaded CAC**

Chemical composition	Weight%	
	Blank	DBT loaded
Carbon	81.87	77.18
Oxygen	11.08	11.40
Aluminum	02.82	03.44
Iron	00.45	01.79
Sulfur	00.27	0.54

**Table 4.1(b). Elemental composition of blank and DBT loaded AICAC**

Chemical composition	Weight%	
	Blank	DBT loaded
Carbon	83.87	69.47
Oxygen	9.09	14.40
Aluminum	1.90	2.89
Iron	1.09	1.21
Sulfur	0.32	0.40

**Table 4.2 Process parameters and their levels for Adsorptive desulfurization by using CAC and AICAC**

Variable, unit	Factors	Level				
		-2	-1	0	1	2
Concentration(mg/l)	X1	100	300	500	700	900
Adsorbent dosage(g/l)	X2	2	7	12	17	22
Time of adsorption(min)	X3	15	195	375	555	735
Temperature(°C)	X4	10	20	30	40	50

**Table 4.3(a) Full factorial design used for Adsorptive desulfurization by using CAC**

Std. order	Run order	C <sub>0</sub> (X1)	m (X2)	t (X3)	T (X4)	Percentage Removal
1	15	300	7	195	20	13.97
2	27	700	7	195	20	6.79
3	29	300	17	195	20	35.86
4	11	700	17	195	20	5.13
5	17	300	7	555	20	27.64
6	30	700	7	555	20	4.45
7	23	300	17	555	20	42.67
8	25	700	17	555	20	3.81
9	6	300	7	195	40	14.71
10	3	700	7	195	40	12.24
11	24	300	17	195	40	32.79
12	28	700	17	195	40	18.37
13	1	300	7	555	40	13.93
14	21	700	7	555	40	7.56
15	7	300	17	555	40	31.78
16	5	700	17	555	40	15.77
17	10	100	12	375	30	45.07
18	2	900	12	375	30	4.10
19	18	500	2	375	30	24.36
20	12	500	22	375	30	41.60
21	4	500	12	15	30	12.37
22	20	500	12	735	30	17.40
23	16	500	12	375	10	25.27
24	13	500	12	375	50	24.00
25	14	500	12	375	30	33.83
26	26	500	12	375	30	33.83
27	9	500	12	375	30	33.83
28	8	500	12	375	30	33.83
29	19	500	12	375	30	33.83
30	22	500	12	375	30	33.83

**Table 4.3(b) Full factorial design used for Adsorptive desulfurization by using AICAC**

Std. order	Run order	$C_0(X1)$	$m(X2)$	$t(X3)$	$T(X4)$	Percentage Removal
1	15	300	7	195	20	16.12
2	27	700	7	195	20	6.78
3	29	300	17	195	20	37.59
4	11	700	17	195	20	4.30
5	17	300	7	555	20	28.25
6	30	700	7	555	20	5.62
7	23	300	17	555	20	45.59
8	25	700	17	555	20	4.39
9	6	300	7	195	40	14.27
10	3	700	7	195	40	13.38
11	24	300	17	195	40	31.12
12	28	700	17	195	40	18.16
13	1	300	7	555	40	14.52
14	21	700	7	555	40	6.32
15	7	300	17	555	40	33.52
16	5	700	17	555	40	16.25
17	10	100	12	375	30	48.62
18	2	900	12	375	30	5.27
19	18	500	2	375	30	23.59
20	12	500	22	375	30	43.19
21	4	500	12	15	30	12.50
22	20	500	12	735	30	18.29
23	16	500	12	375	10	26.17
24	13	500	12	375	50	25.63
25	14	500	12	375	30	33.83
26	26	500	12	375	30	33.83
27	9	500	12	375	30	33.83
28	8	500	12	375	30	33.83
29	19	500	12	375	30	33.83
30	22	500	12	375	30	33.83



**Table 4.4(a). Adequacy of the models tested for desulfurization by CAC.**

Source	Sum of Squares	DF <sup>1</sup>	Mean Square	F Value	Prob > F	Remark
<b>Sequential Model Sum of Squares</b>						
Mean	15630.22	1	15630.22			
Linear	2646.10	4	661.526	7.86	0.0003	
2FI	574.44	6	95.74	1.19	0.3526	
Quadratic	1237.62	4	309.40	16.03	< 0.0001	Suggested
Cubic	75.41	8	9.42	0.308	0.9393	Aliased
Residual	213.93	7	30.56			
Total	20377.75	30	679.25			
Source	Std. Dev.	Predicted R <sup>2</sup>	Adjusted R <sup>2</sup>	R <sup>2</sup>	PRESS	Remark
<b>Model Summary Statistics</b>						
Linear	9.168	0.557	0.486	0.383	2925.305	
2FI	8.964	0.678	0.509	0.205	3769.694	
Quadratic	<u>4.392057</u>	<u>0.939052</u>	<u>0.882167</u>	<u>0.648939</u>	<u>1666.67</u>	<u>Suggested</u>
Cubic	5.528	0.954	0.813	-5.488	30806.44	Aliased

<sup>1</sup>DF: Degree of Freedom

**Table 4.4(b). Adequacy of the models tested for desulfurization by AICAC.**

Source	Sum of Squares	DF <sup>1</sup>	Mean Square	F Value	Prob > F	Remark
<b>Sequential Model Sum of Squares</b>						
Mean	16455.8	1	16455.8			
Linear	2926.12	4	731.53	8.611	0.0002	
2FI	658.76	6	109.794	1.423	0.2569	
Quadratic	1146.63	4	286.65	13.507	< 0.0001	Suggested
Cubic	64.42	8	8.053	0.222	0.9746	Aliased
Residual	253.91	7	36.273			
Total	21505.67	30	716.85			
Source	Std. Dev.	Predicted R <sup>2</sup>	Adjusted R <sup>2</sup>	R <sup>2</sup>	PRESS	Remark
<b>Model Summary Statistics</b>						
Linear	9.216	0.406	0.512	0.579	2997.84	
2FI	8.780	0.266	0.557	0.709	3703.057	
Quadratic	<u>4.606794</u>	<u>0.936961</u>	<u>0.878125</u>	<u>0.636896</u>	<u>1833.629</u>	<u>Suggested</u>
Cubic	6.022	6.240	0.791	0.949	36563.36	Aliased

<sup>1</sup>DF: Degree of Freedom

**Table 4.5(a). ANOVA for Response Surface Quadratic Model (for CAC).**

Source	Coefficient Estimate	Sum of Squares	DF <sup>1</sup>	Mean Square	F Value	Prob > F	Remark
<b>Model</b>		4458.17	14	318.44	16.50	< 0.0001	Highly significant
Intercept	33.83						
X1	-9.21	2038.26	1	2038.26	105.66	< 0.0001	Highly significant
X2	4.97	593.85	1	593.85	30.78	< 0.0001	Highly significant
X3	0.74	13.21	1	13.21	0.685	0.4208	
X4	0.178	0.765	1	0.765	0.039	0.8447	
X1 <sup>2</sup>	-3.36	310.06	1	310.06	16.07	0.0011	significant
X2 <sup>2</sup>	-1.26	43.81	1	43.81	2.271	0.1526	
X3 <sup>2</sup>	-5.78	918.62	1	918.62	47.62	< 0.0001	Highly significant
X4 <sup>2</sup>	-3.35	307.95	1	307.95	15.96	0.0012	significant
X1 × X2	-3.80	231.05	1	231.05	11.97	0.0035	significant
X1 × X3	-1.85	54.86	1	54.86	2.84	0.1124	Low significant
X1 × X4	3.793	230.23	1	230.23	11.93	0.0035	significant
X2 × X3	-0.24	0.990	1	0.990	0.051	0.8238	
X2 × X4	0.979	15.35	1	15.35	0.795	0.3864	
X3 × X4	-1.619	41.95	1	41.95	2.174	0.1610	
Residual		289.35	15	19.29			
<i>Lack of fit</i>		289.35	10	28.93			
<i>Pure Error</i>		0	5	0			
Cor Total		4747.52	29				

<sup>1</sup>DF: Degree of Freedom

**Table 4.5(b). ANOVA for Response Surface Quadratic Model (AICAC).**

Source	Coefficient Estimate	Sum of Squares	DF <sup>1</sup>	Mean Square	F Value	Prob > F	Remark
<b>Model</b>		4731.53	14	337.96	15.92	< 0.0001	Highly Significant
Intercept	33.83						
X1	-9.68	2251.68	1	2251.68	106.09	< 0.0001	Highly Significant
X2	5.20	649.56	1	649.56	30.60	< 0.0001	Highly Significant
X3	1.014	24.68	1	24.68	1.163	0.2979	
X4	-0.090	0.196	1	0.196	0.0092	0.9245	Not Significant
X1 <sup>2</sup>	-2.87	226.01	1	226.01	10.65	0.0052	
X2 <sup>2</sup>	-1.26	43.57	1	43.57	2.053	0.1724	
X3 <sup>2</sup>	-5.75	909.22	1	909.22	42.84	< 0.0001	Highly Significant
X4 <sup>2</sup>	-3.13	269.00	1	269.00	12.67	0.0028	Significant
X1 × X2	-3.97	253.25	1	253.25	11.93	0.0035	Significant
X1 × X3	-2.05	67.32	1	67.32	3.172	0.0951	
X1 × X4	4.196	281.78	1	281.78	13.27	0.0024	Significant
X2 × X3	0.275	1.214	1	1.214	0.057	0.8142	Not Significant
X2 × X4	0.966	14.943	1	14.94	0.704	0.4146	
X3 × X4	-1.585	40.24	1	40.24	1.896	0.1887	
Residual		318.33	15	21.22			
<i>Lack of Fit</i>		318.33	10	31.83			
<i>Pure Error</i>		0	5	0			
Cor Total		5049.86	29				

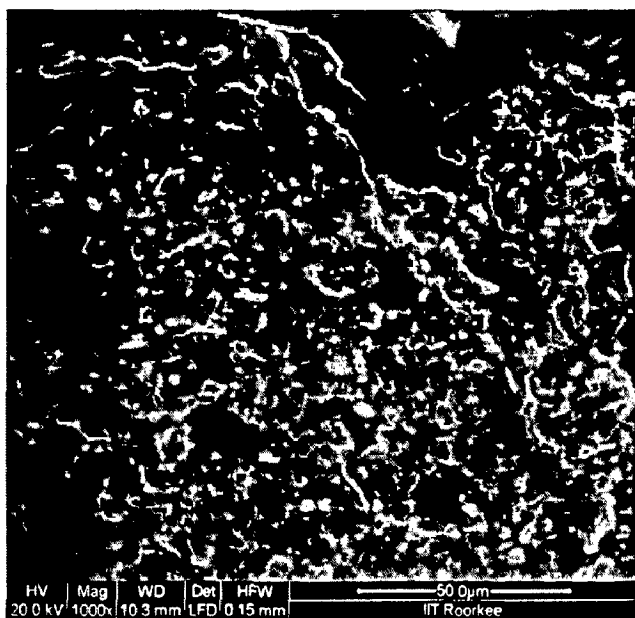
<sup>1</sup>DF: Degree of Freedom

**Table 4.6 Isotherm parameters for the removal of DBT by Activated carbon ( $t = 6$  h,  $C_0 = 50$ -1000 mg/l,  $m = 20$  g/l).**

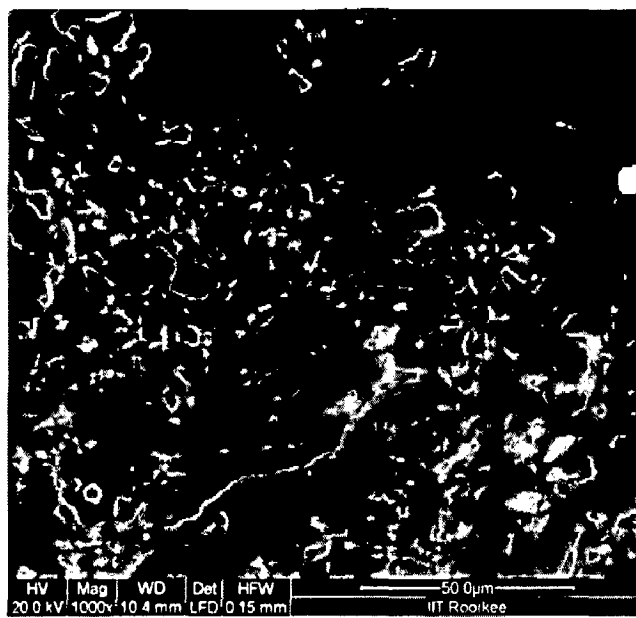
Isotherms	Constants	GAC		
		Temperature (K)		
		288	303	318
<b>Langmuir</b> $q_e = \frac{q_m K_L C_e}{1 + K_L C_e}$	$K_L$ (L/mg)	0.0149	0.0079	0.0094
	$q_m$ (mg/g)	6.49	9.95	11.67
	$R^2$ (non-linear)	0.967	0.966	0.969
	MPSD	35.34	45.34	46.02
<b>Freundlich</b> $q_e = K_F C_e^{1/n}$	$K_F$ (L/mg)	0.338	0.382	0.397
	$1/n$	0.733	0.765	0.873
	$R^2$ (non-linear)	0.994	0.983	0.983
	MPSD	10.09	14.53	39.32
<b>Temkin</b> $q_e = \frac{RT}{b} \ln(K_T C_e)$	$B_1$	0.836	1.09	1.49
	$K_T$ (L/mg)	1.13	1.13	0.87
	$R^2$ (non-linear)	0.953	0.938	0.947
	MPSD	19.89	19.48	25.42
<b>Redlich-Peterson</b> $q_e = \frac{K_R C_e}{1 + a_R C_e^B}$	$a_R$ (L/mg)	5917.65	1653.76	2932.55
	$K_R$ (L/mg)	4339.64	1266.33	2785.66
	$B$	0.661	0.617	0.617
	$R^2$ (non-linear)	0.994	0.983	0.986
	MPSD	10.10	14.54	40.43

**Table 4.7 Thermodynamics parameters for the adsorption of DBT by CAC ( $t = 6$  h,  $C_0 = 50$ -1000 mg/l,  $m = 20$  g/l).**

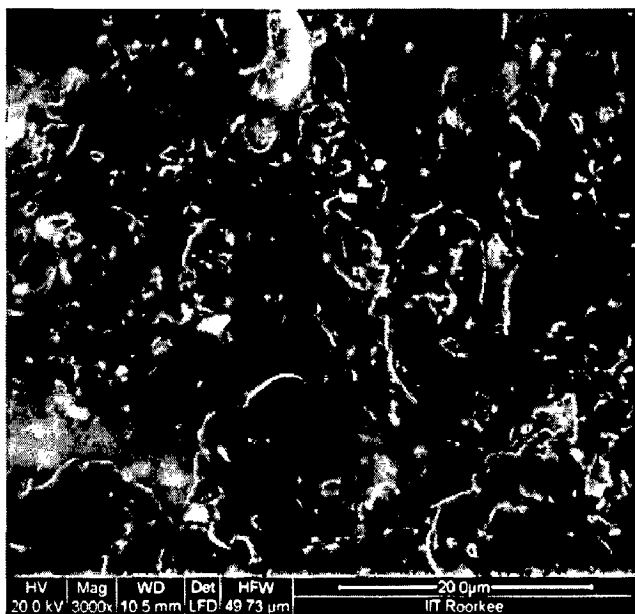
Temp. (K)	$K \times 10^{-3}$ (l/kg)	$\Delta G^0$ (kJ/mol)	$\Delta H^0$ (kJ/mol)	$\Delta S^0$ (kJ/mol K)
288	548.1903	-15.1092	9.7471	85.9188
303	589.9336	-16.0807		
318	807.9887	-17.7084		



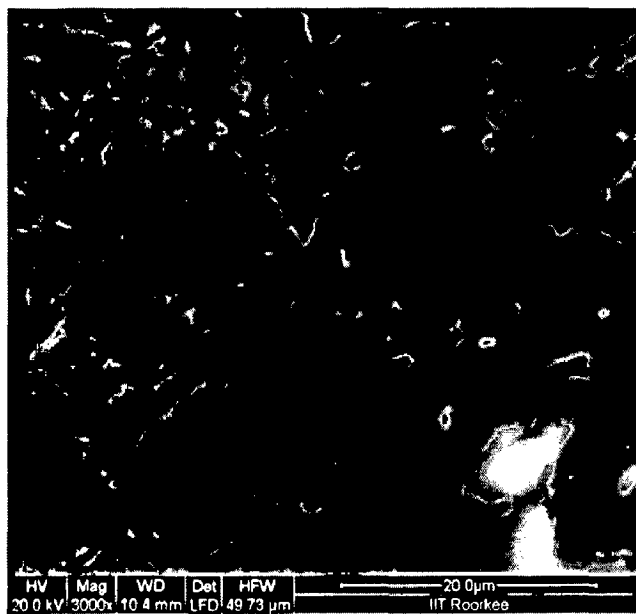
**CAC (1000X)**



**DBT loaded CAC (1000X)**

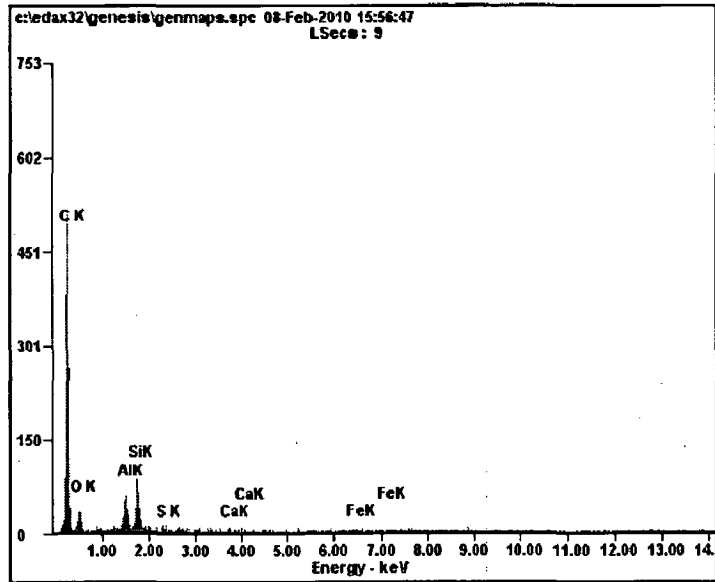


**AICAC (3000X)**

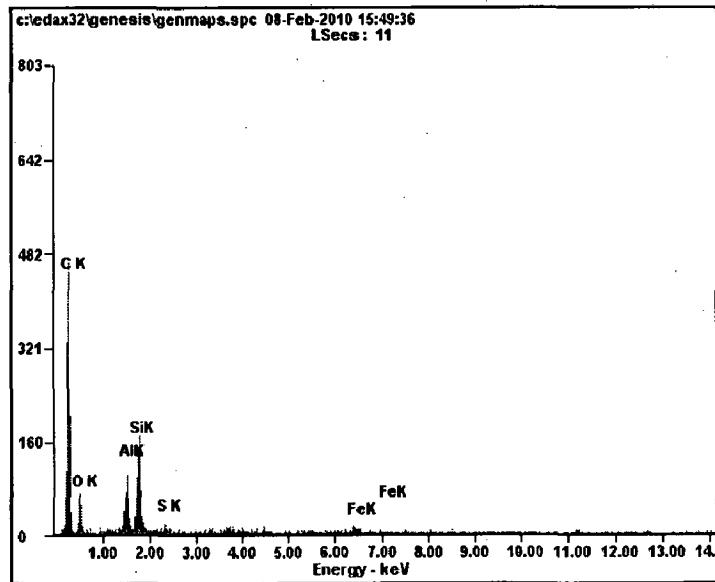


**DBT loaded AICAC (3000X)**

**Fig. 4.1 Scanning electron micrograph of blank and DBT loaded CAC and AICAC.**

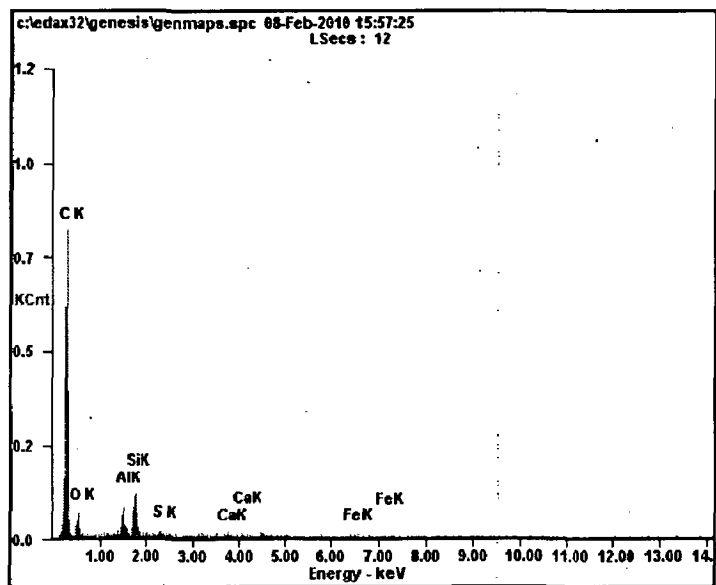


**Blank CAC**

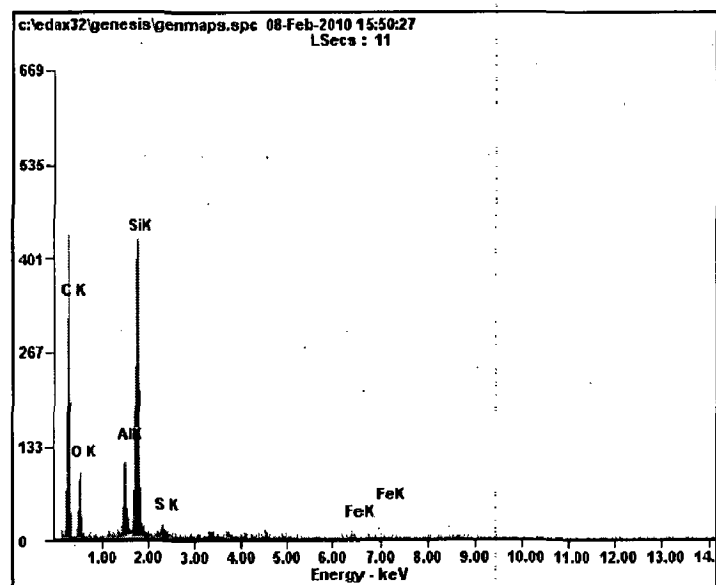


**DBT loaded CAC**

**Fig. 4.2(a) EDX of Blank and DBT loaded CAC**



**Blank AICAC**



**DBT loaded AICAC**

**Fig. 4.2(b) EDX of Blank and DBT loaded AICAC**



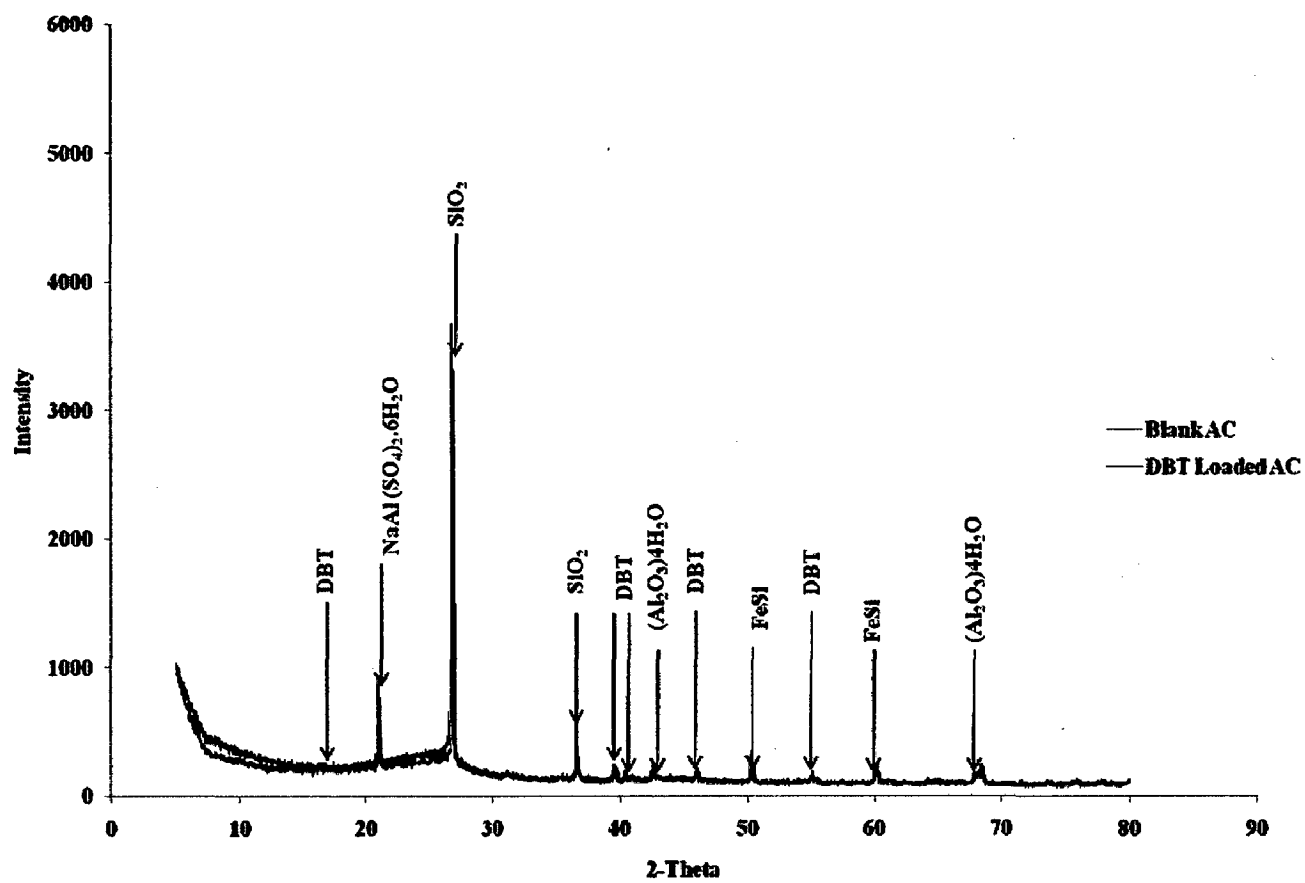
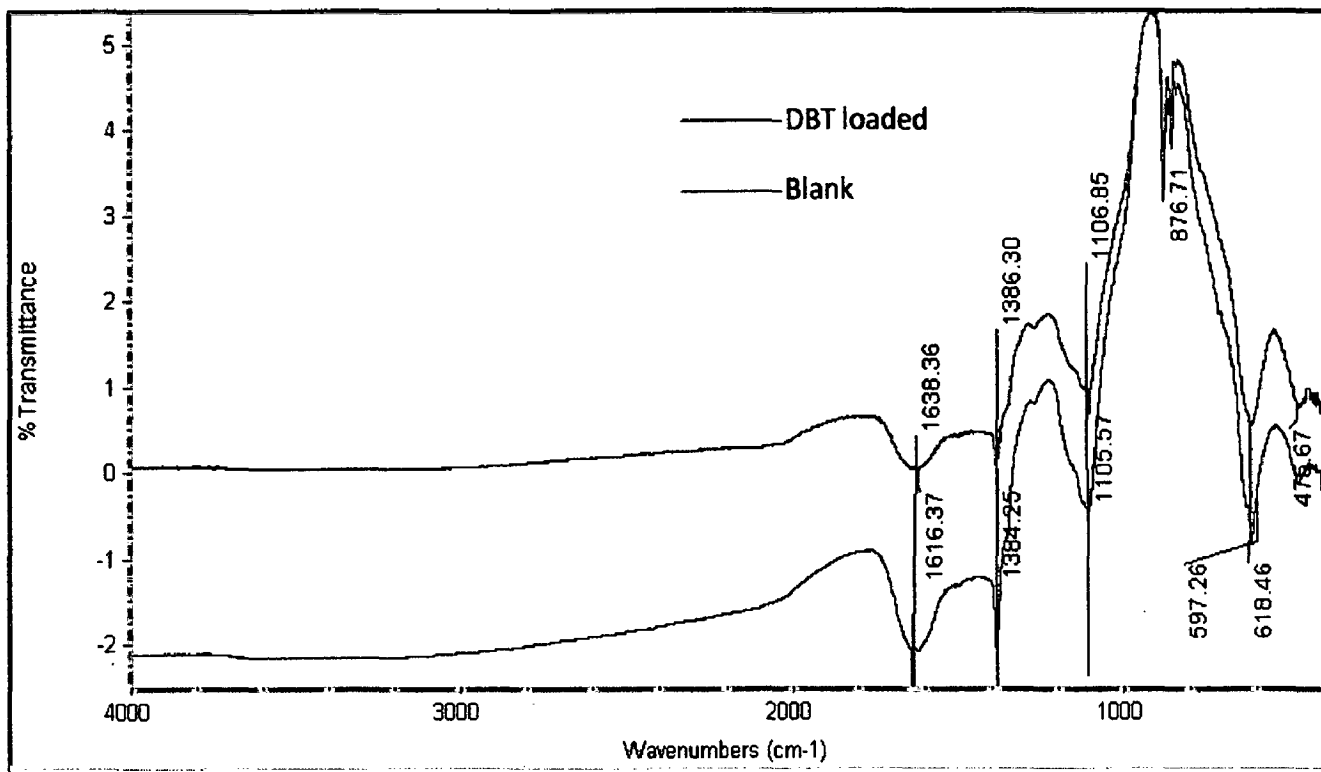
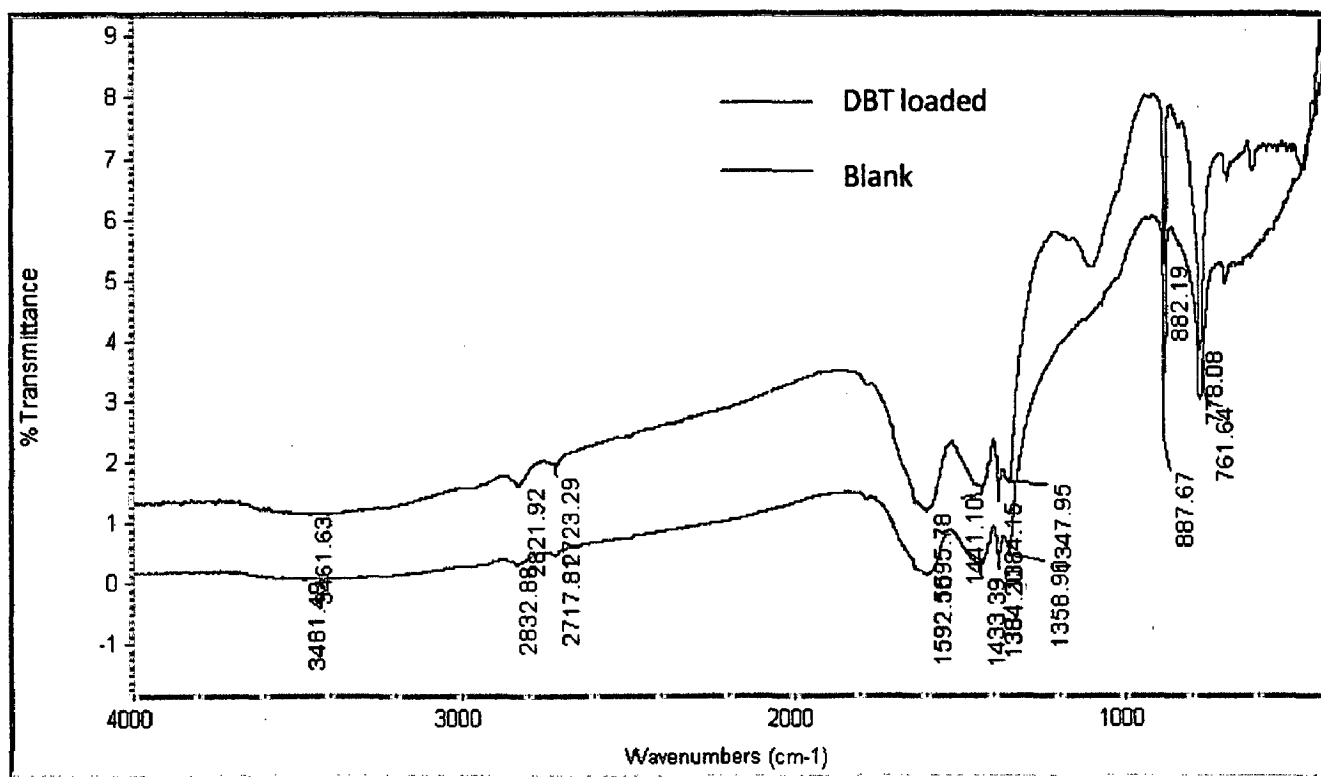


Fig 4.3 XRD spectra of blank and DBT loaded CAC



**Fig. 4.4(a) FTIR spectra of blank and DBT loaded CAC**



**Fig. 4.4(b) FTIR spectra of blank and DBT loaded AICAC**

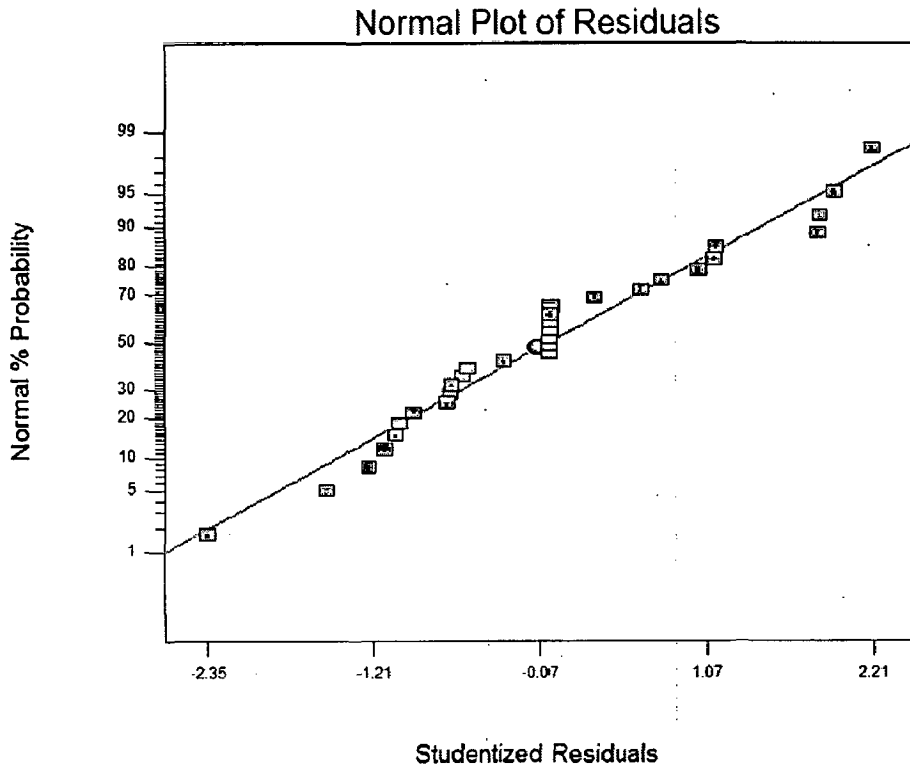


Fig. 4.5(a). Normal % probability versus residual error (for CAC).

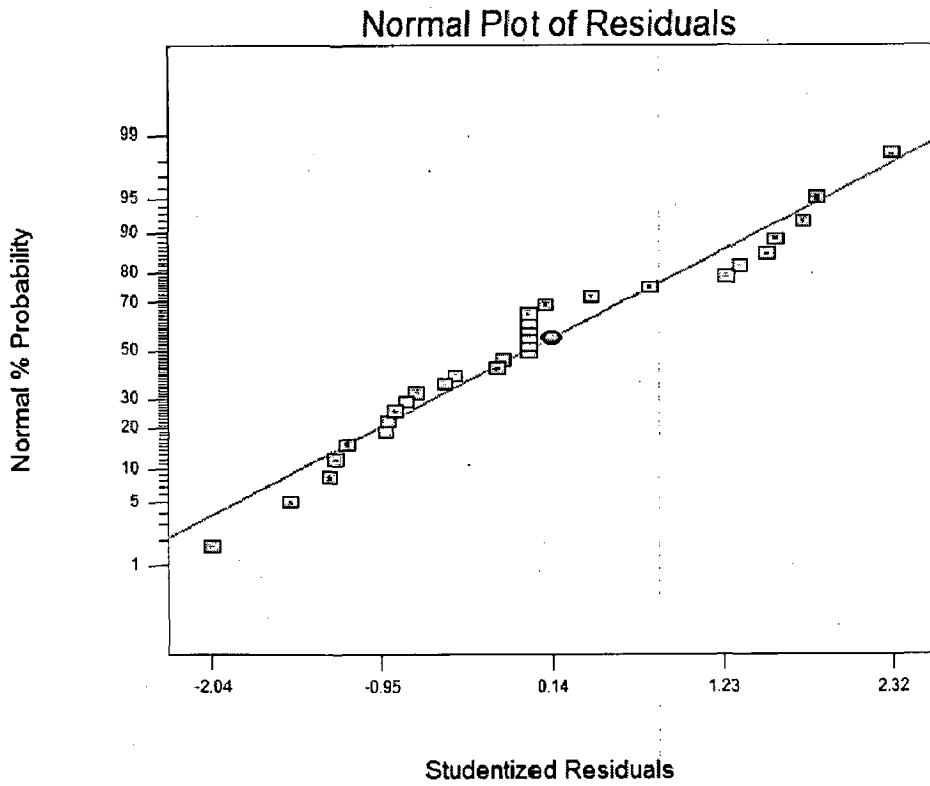
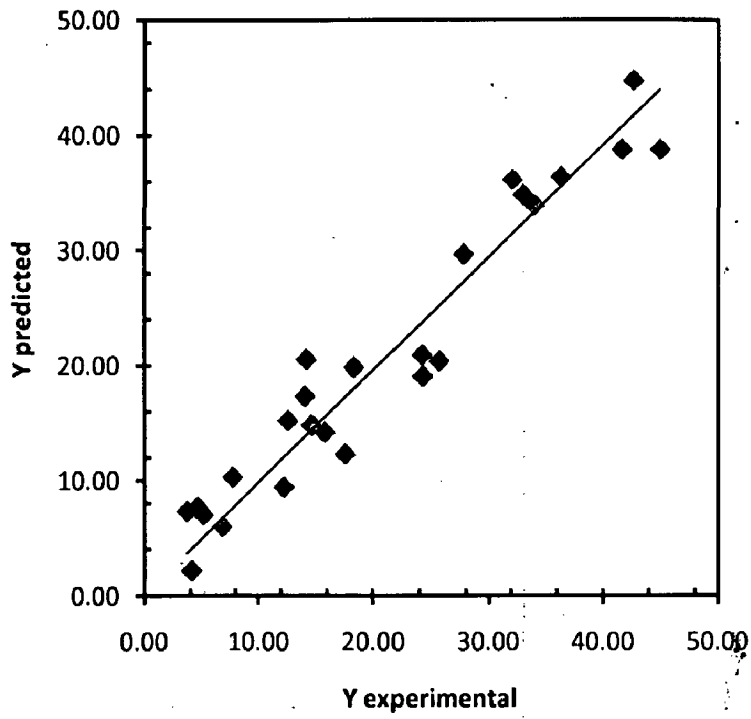
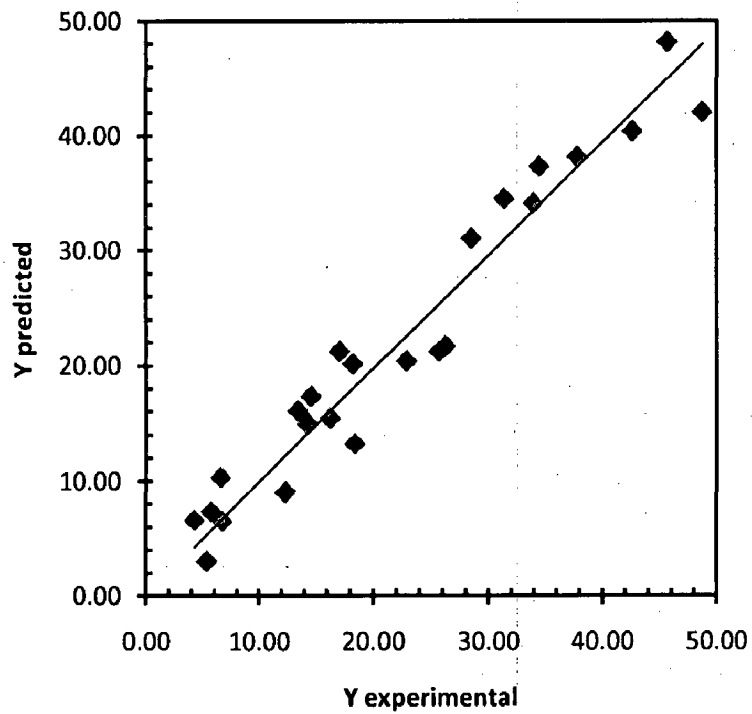


Fig. 4.5(b) Normal % probability versus residual error (for AICAC).



**Fig. 4.6(a) Scatter diagram of predicted response versus actual response for adsorption of DBT onto CAC.**



**Fig. 4.6(b) Scatter diagram of predicted response versus actual response for adsorption of DBT onto AICAC.**

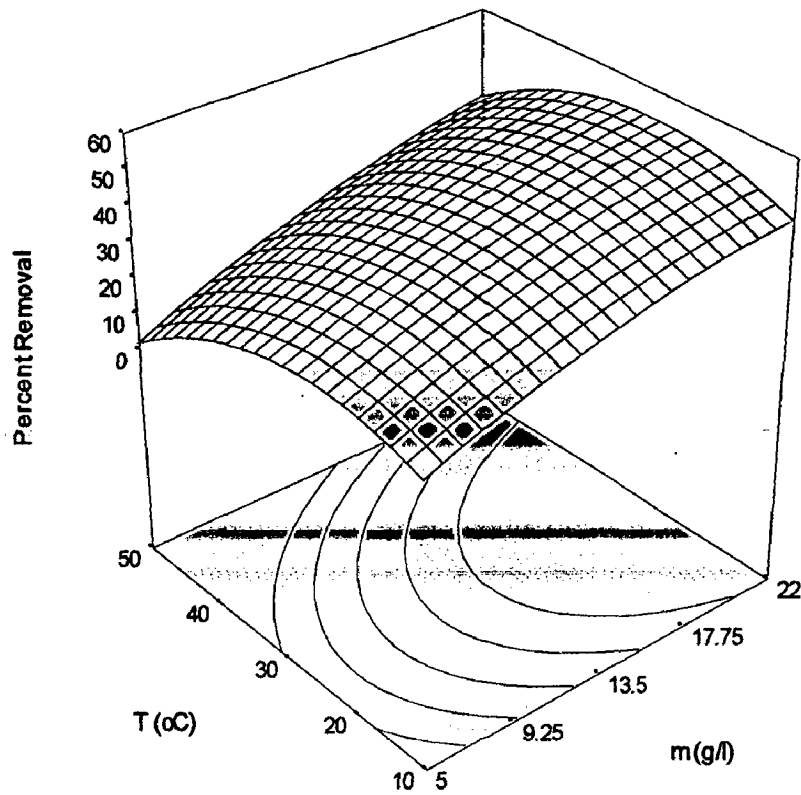


**Fig. 4.7(a) 3D response graph for DBT removal versus adsorbent dose and temperature (for CAC)**

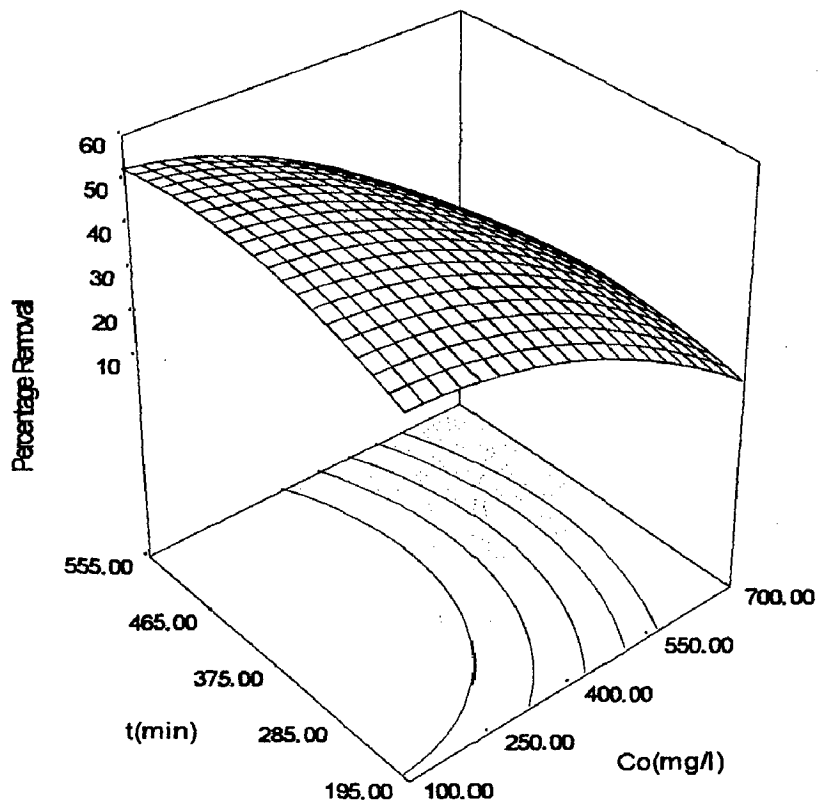


**Fig. 4.7(b) 3D response graph for DBT removal versus concentration and time (for CAC)**

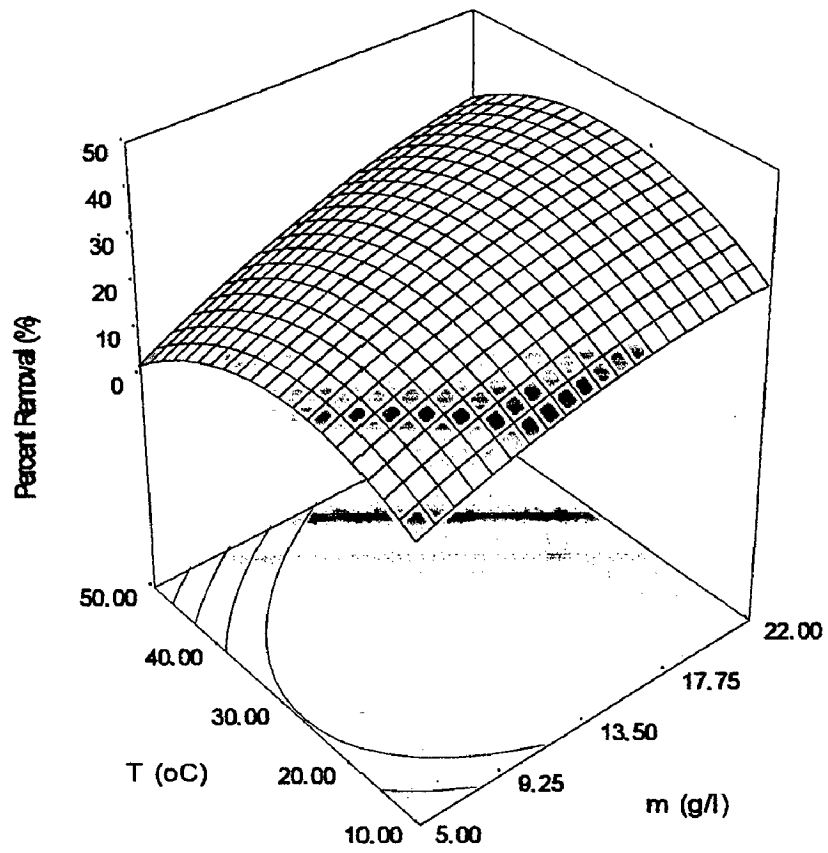


**Fig. 4.8(a) 3D response graph for DBT removal versus adsorbent dose and temperature (for AICAC)**

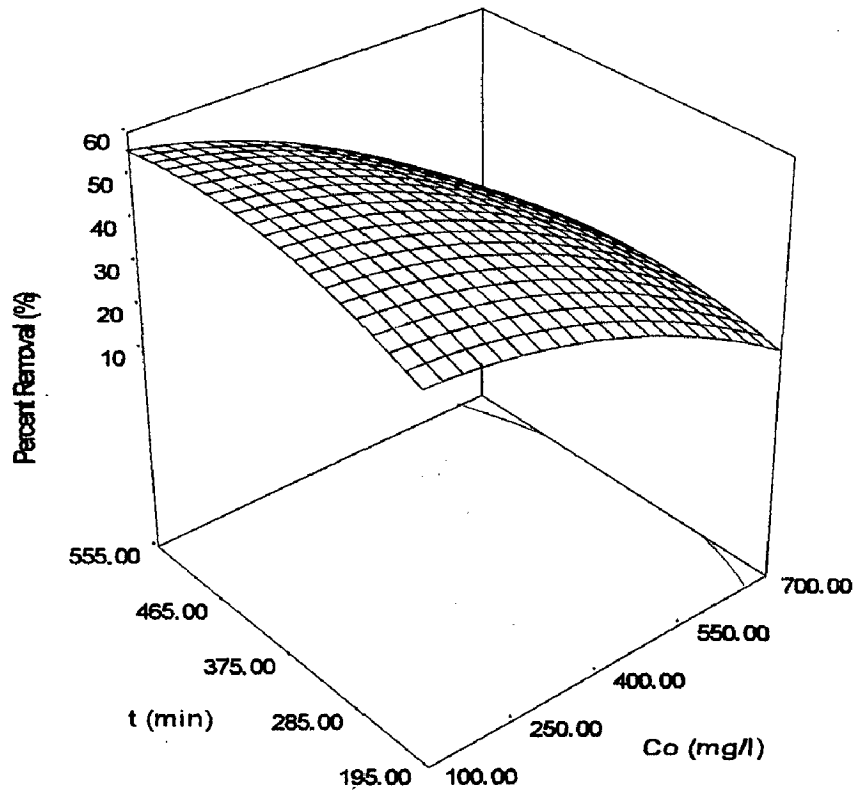


**Fig. 4.8(b) 3D response graph for DBT removal versus concentration and time (for AICAC)**

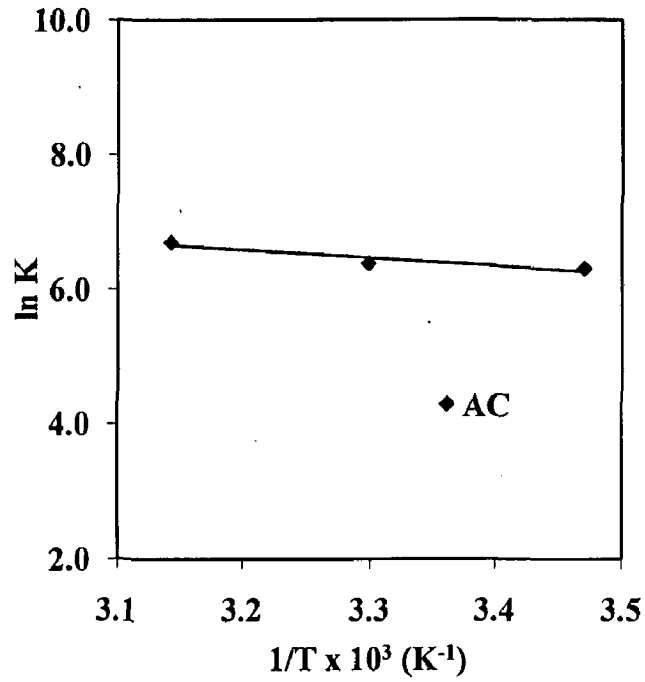


Fig. 4.9 The van't Hoff plot for the Redlich-Peterson isotherm

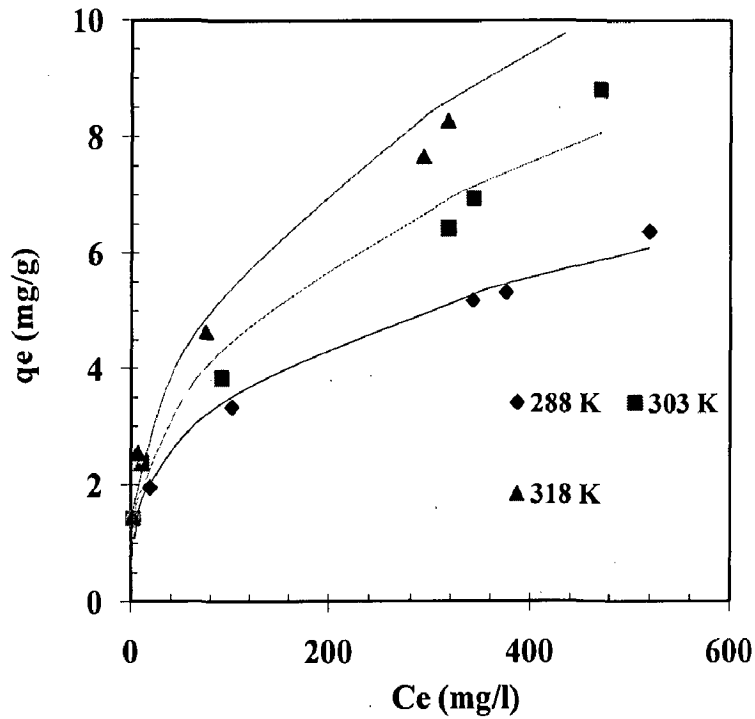


Fig 4.10 Equilibrium adsorption isotherms at different temperature for DBT CAC system,  $t = 6$  h,  $C_0 = 50-1000$  mg/l,  $m = 20$  g/l. Experimental best data points given by the symbols and the lines predicted by Redlich-Peterson equation.

## CHAPTER 5 *CONCLUSIONS AND RECOMMENDATIONS*

---

### 5.1 CONCLUSIONS

In the present study, commercial activated carbon (CAC) and alum impregnated commercial activated carbon (AICAC) were characterized by various techniques were used for removal sulfur from model oil (dibenzothiophene (DBT) dissolved in iso-octane). Central composite design was used for optimization of parameters namely initial concentration ( $C_0= 100-900$  mg/l), adsorbent dosage ( $m= 2-22$  g/l), time ( $t= 15-735$  min), and temperature ( $T= 10-50$  °C).

The following major conclusions have been drawn from the present work.

1. The FTIR spectra of the adsorbents indicated the presence of various types of functional groups.
2. The morphologies of blank and DBT loaded CAC and AICAC were examined under scanning electron microscope (SEM).
3. Percent removal of DBT increased with an increase in the adsorbent dose of CAC and AICAC. Adsorbent dose of 20 g/l was found to be optimum for both the adsorbents.
4. The percent removal of DBT by both adsorbents decreased with an increase in initial concentration ( $C_0$ ).
5. Adsorption capacity of CAC for DBT removal decreased with an increase in temperature showing the endothermic nature of adsorption.
6. Redlich-Peterson isotherm best-fitted the isotherm data for DBT adsorption onto CAC.
7. The results proved that both the adsorbents are suitable for DBT removal with AICAC giving greater removal than CAC.



## **5.2 RECOMMENDATIONS**

On the basis of the present studies, the following recommendations may be made for future studies:

1. Various metal impregnated CACs could be checked for the DBT removal from model oil.
2. Adsorption column studies should be carried out for DBT-activated system at different inlet concentration, flow rates, bed heights and column diameter to get the characteristic dependence of the adsorption capacity and other parameters. Design parameter for scaled up adsorption column should, thereafter, be fixed for the removal of sulfur compounds from gasoline.
3. Adsorption studies should be carried out using blank and metal-loaded CAC for the removal of sulfur from actual liquid fuels to test their efficacy for sulfur removal.

## REFERENCES

---

1. Ali MH, Al-Maliki A, El-Ali B, Martine G, Siddiqui MN. Deep desulfurization of gasoline and diesel fuels using non-hydrogen consuming techniques. *Fuel*. 2006; 85: 1354-1363.
2. Alves L, Marque S, Matos J, Tenreiro R, girio FM. Dibenzothiophene desulfurization by gordonia alkanivorans strain 1B using recycled paper sludge hydrolyzate. *Chemosphere*. 2008; 70: 967-973.
3. Ania CO, Parra JB, Arenillas A, Rubiera F, Bandosz TJ, Pis JJ. On the mechanism of reactive adsorption of dibenzothiophene on organic waste derived carbons. *Applied Surface Science* 2007; 253: 5899-5903.
4. Ankur Srivastav, Vimal Chandra Srivastava, Adsorptive desulfurization by activated alumina. *Journal of Hazardous Materials* 170 (2009) 1133-1140.
5. Annual Energy Review. Energy Dept., Energy Information Administration, Office of Energy Markets and End Use. DOE/EIA-0384. 2004.
6. Antonio C, Avelino C, Marcelo E. Catalytic oxidative desulfurization (ODS) of diesel fuel on a continuous fixed-bed reactor. *Journal of Catalysis*. 2006; 242: 299-308.
7. Arias M, Laurenti D, Geantet C, Vrinat M, Hideyuki I, Yoshimura Y. Gasoline desulfurization by catalytic alkylation over silica-supported heteropolyacids: From model reaction to real feed conversion. *Catalysis Today* 2008; 130: 190-194.
8. Attar A, Corcoran WH. Desulfurization of sulfur compounds by. Selective oxidation. *Ind Eng. Chenz. Prod. Res. Dev.* 1978; 17: 102-109.
9. Audeh CA. Process of reducing sulfur content in crude. USA patent 5310479, 1994.
10. Baeza P, Aguila G, Gracia F, Araya P. Desulfurization by adsorption with copper supported on zirconia. *Catalysis Communications* 2008; 9: 751-755.
11. Bagreev Andrey, Sai Katikanenib, Sanjay Parabb, Teresa J. Bandosza, Desulfurization of digester gas: prediction of activated carbon bed performance at low concentrations of hydrogen sulfide. *Catalysis Today* 99 (2005) 329-337.
12. Baldovino-Medrano VG, Giraldo SA, Centeno A. The functionalities of Pt/ $\gamma$ - $\text{Al}_2\text{O}_3$  Catalysts in simultaneous HDS and HAD reactions. *Fuel* 2008; 87: 1917-1926.

13. Bezverkhyy I, Ryzhikov A, Gadacz G, Bellat JP. Kinetics of thiophene reactive adsorption on Ni/SiO<sub>2</sub> and Ni/ZnO. *Catalysis Today*. 2008; 130: 199-205.
14. Bhatia S, Sharma DK. Biodesulfurization of dibenzothiophene, its alkylated derivatives and crude oil by a newly isolated strain *Pantoea agglomerans* D23W3. *Biochemical Engineering Journal*. 2010; 50: 104–109.
15. Blumberg Ko, Walsh MP, Pera C. Low-sulfur gasoline & diesel: The key to lower vehicle emissions. William and Flora Hewlett Foundation for the International Council on clean Transportation (ICCT).2003.
16. CAI-Asia, Summary of country/city synthesis reports across asia. 2006.
17. Caro A, Leton P, Garcia-Calvo E, Setti L. R Enhancement of dibenzothiophene biodesulfurization using  $\beta$ -cyclodextrins in oil-to-water media. *Fuel*. 2007; 86: 2632-2636.
18. Chan K, Jung J, Lee J, Sang B, Kyungil C, Moon Sh. Hydrodesulfurization of DBT,4-MDBT and 4,6-DMDBT on fluorinated CoMoS/Al<sub>2</sub>O<sub>3</sub> Catalysts. *Applied Catalysis A: General*. 2000; 200: 233-42.
19. Chen H, Zhang WJ, Chen JM, Cai YB, Li W. desulfurization of various organic sulfur compounds and the mixture of DBT +4, 6-DMDBT by *Mycobacterium* sp.ZD-19. *Bioresource Technology*.2007; 99: 3630-3634.
20. Collins FM, Lucy AR, Sharp C. Oxidative desulphurization of oils via hydrogen peroxide and heteropolyanion catalysis. *J. Mol. Catal*. 1997; 117: 397-403.
21. Dehaghani FD, Manouchehr V, Abed AZ. Biodesulfurization of dibenzothiophene by a newly isolated *Rhodococcus erythropolis* strain. *Bioresource Technology*. 2010; 101: 1102–1105.
22. Deng Z, Tiefeng W, Zhanwen W. Hydrodesulfurization of diesel in a slurry reactor. *Chemical Engineering Science*. 2010; 65: 480 – 486.
23. Dolbear GE, Skov ER. Selective oxidation as a route to petroleum desulfurization. *Am. Chem. Soc. Div. Fuel. Chem*. 2000, 45: 375-378.
24. Emison GA. Sir Quality analysis for prevention of significant deterioration. United States Environmental protection Agency, Office of Air Quality Planning and Standards, 2000.

25. Energy Information Administration. The transition to ultra low sulfur diesel fuel: Effects on prices and supply, Washington DC. 2001.
26. Etemadi O, Yen TF. Surface characterization of adsorbents in ultrasound-assisted oxidative desulfurization process of fossil fuels. *Journal of Colloid and Interface Science* 2007; 313: 18-25.
27. Fang WL. Inventory of U.S. Greenhouse gas emissions and sinks: 1990-2003. Clean Air Markets Division. 2004.
28. Farag H, Isao M, Kinya S. Fundamental comparison studies on hydrodesulfurization of dibenzothiophenes over CoMo-based carbon and alumina catalysts. *Applied Catalysis A: General*. 2000; 194–195: 147–157.
29. Frances MC, Anderw RL, Christopher S. Oxidative desulfurization of oils via hydrogen peroxide and heteropolyanion. *Journal of molecular catalysis A; chemical* 1997; 117: 397-403.
30. Gongshin Q. New nano-structured materials for NO/NH<sub>3</sub> abatement desulfurization and hydrogen storage. University of Michigan 2006.
31. Grassman MJ, Siskin M, Ferrughelli DT, Lee MK. Method for removal of organic sulfur from carbonaceous material. USA patent. 1999; 5910440.
32. Haji S. Desulfurization of Diesel for Fuel Cell Application. University of Connecticut. 2005.
33. Heeyeon k, Jung J, Lee S, Heup M, Hydrodesulfurization of DBT compounds using fluorinated NiMo/Al<sub>2</sub>O<sub>3</sub> catalysts. *Applied catalysis B; Environmental*. 2003; 44: 287-299.
34. Hernandez A.J., R.T. Yang, New sorbents for desulfurization by selective adsorption via pi-complexation: sulfur removal from diesel fuels, *AIChE J.* 50 (2004) 791-801.
35. Hou Y, Ying K, Jinrong Y, Jianhui Z, Deqing S, Wei X. Biodesulfurization of dibenzothiophene by immobilized cells of *Pseudomonas stutzeri* UP-1. *Fuel*. 2005; 84: 1975–1979.
36. Houalla M, Broderick DH, Sapre AV, Nag NK, Beer VHJD. Hydrodesulfurization of methyl substituted DBTs catalyzed by sulfide CoO-MoO<sub>3</sub>/γ-Al<sub>2</sub>O<sub>3</sub>. *J. Catal.* 1980; 61: 523.

37. Houalla M, Nag NK, Sapre AV, Broderick DH, Gates BC. Hydrodesulfurization of DBT catalyzed by sulfide CoO-MoO<sub>3</sub>/γ-Al<sub>2</sub>O<sub>3</sub>: The reaction network *AIChE J.* 1978; 24: 1015.
38. <http://www.epa.gov/sbrrefaldocuments/pnl13f.pdf>
39. James GH, Handewerk GE. *Petroleum Refining: Technology and Economics*, Second Edition, Marcel Dekker, New York. 1984.
40. Jeyagowry TS, Xiao H, Dou J, Nah TY, Rong X, Kwan WP. A novel oxidative desulfurization process to remove refractory sulfur compounds from diesel fuel. *Applied Catalysis B: Environmental.* 2006; 63: 85–93.
41. Jianghua Q, Guanghui W, Danlin Z, Yan T, Meng W, Yanjun L. Oxidative desulfurization of diesel fuel using amphiphilic quaternary ammonium phosphomolybdate catalysts. *Fuel Processing Technology.* 2009; 90: 1538–1542.
42. Jindal S, *Vehicular Pollution Control – Indian Perspective and Future Strategies*, Ministry of Environment & Forests- Government of India. 2004.
43. Kabe T, Yasuo A, Danhong W, Atsushi I, Weihua Q, Masataka H, Qin Z. Effects of H<sub>2</sub>S on hydrodesulfurization of dibenzothiophene and 4,6-dimethyldibenzothiophene on alumina-supported NiMo and NiW catalysts. *Applied Catalysis A: General.* 2001; 209: 237–247.
44. Kalhe GS. *Vehicle Technology and Fuel Quality in India. Partnership for Clean Fuels and Vehicles*, New Delhi. 2006.
45. Kemp DA. Fuel standard (Autogas) determination. European Committee for standardization. 2003.
46. Kim J.H., X. Ma, A. Zhou, C. Song, Ultra-deep desulfurization and denitrogenation of diesel fuel by selective adsorption over three different adsorbents: A study on adsorptive selectivity and mechanism, *Catal. Today* 111 (2006) 74-83.
47. Klimova T, Reyes J, Gutierrez O, Lizama L. Novel bifunctional NiMo/Al-SBA-15 catalysts for deep hydrodesulfurization: Effect of support Si/Al ratio. *Applied catalysis A: General.* 2008; 335: 159-171.
48. Koch TA, Krause KR, Manzer LE, Mehdizadeh M, Odom JM, Sengupta SK, *New J. Chem.* 1996; 20: 163-173.

49. Kwak C, Jung J, Sang B, Kyungil C, Sang H. Hydrodesulfurization of DBT, 4-MDBT, and 4,6-DMDBT on fluorinated CoMoS/Al<sub>2</sub>O<sub>3</sub> catalysts. *Applied Catalysis A: General*. 2000; 200: 233–242.
50. Lanju C, Shaohui GUO, dishun ZHAO. Oxidative desulfurization of simulated gasoline over metal oxide-loaded molecular sieve. *Chin. J. Chem. Eng.* 2007; 15(4): 520-523.
51. Larrubia MA, Gutierrez-Alejandre A, Ramirez J, Busca G. A FT-IR study of adsorption of indole, Carbazole, BTH, DBT and 4, 6-dimethyle DBT over solid adsorbents and catalysts. *Appl. Catal. A* 2002; 224: 167.
52. Lee SHD, Kumar R.Krumpeli M.Sulfur removal from diesel fuel contaminated methanol.Sep. Purif. Technol, 2002; 26: 247.
53. Li W, Liu Q, Xing J, Gao H Xiong X, Li Y, Li X Liu H. High-eefficiency desulfurization by adsorption with mesoporous aluminosilicates. *AIChE Journal*.2007; 53(12): 3263-3268.
54. Li W, Liu Q, Xing J, Gao H Xiong X, Li Y, Li X Liu H. High-eefficiency desulfurization by adsorption with mesoporous aluminosilicates. *AIChE Journal*.2007; 53(12): 3263-3268.
55. Liu WY , Leii Zl. Wang IK.Kinetics and mechanism of Plasma Oxidative Desulfurization in Liquid Phase.*Energy Fuels*.2001; 15: 38-43.
56. Lu SH.The feasibility studies for desulfurization of heavy oil by intermetallic adsorption and ultrasonic oxidation.University of Southern California.2000.
57. Ma X, Sun L. Song C. Anew approach to deep desulfurization of gasoline disel and jet fuel by selective adsorption . *Catalysis Today*. 2007; 77: 107.
58. Madeira L, Ferreira-Leitao VS , Bon EPS.Dibenzothiophene oxidation by horseradish peroxidase in organic media: Effect of the DBT: H<sub>2</sub>O<sub>2</sub> molar ratio and H<sub>2</sub>O<sub>2</sub> addition mode. *Chemosphere* 2008: 71: 189-194.
59. McKinley SG.Deep Desulfurization of petroleum feedstock by selective adsorption and extraction. Iowa State University.2003
60. Mei H, Mei BW Yen TF.A new method for obtaining ultra-low sulfur diesel fuel via ultrasound assisted oxidative desulfurization.*Fuel*.2003; 82: 405-414.

61. Meng C, Fang Y, Jin L, Hu H. Deep desulfurization of model gasoline by selective adsorption on Ag<sup>+</sup>/Al-MSU-S. *Catalysis Today*. 2010; 149: 138–142.
62. Michael JG, Bruce CC. Reactivities reaction networks and kinetic in high pressure catalytic hydroprocessing. *Ind. Eng. Chem. Res.* 1991; 30: 2021-2058.
63. Mikhail S, Zaki T, Khalil L. Desulfurization by an economically adsorption technique. *Applied Catalysis A: General*. 2002; 227: 265–278.
64. Mohebali G, Ball AS, Rasekh B, Kaytash A. Biodesulfurization potential of a newly isolated bacterium, *Gordonia alkanivorans* RIPI90A. *Enzyme and Microbial Technology*. 2007; 40: 578-584.
65. Muzic M, Sertic-Biondaa K, Gomzia Z, Podolskib S, Telen S. Study of diesel fuel desulfurization by adsorption. *chemical engineering research and design*. 2010; 88: 487–495.
66. Myers AW, Dong L, Atestin TA, Skugrud R, Laschenriem C, Jones WD. Bond cleavage reactions in substituted thiophenes by a rhodium complex. *Inorganica Chimica Acta*. 2007; In Press.
67. Nehlsen JP. *Developing Clean Fuels: Novel Techniques for desulfurization*, Princeton University, 2006.
68. Ngamcharussrivichai C, Chatratananon C, Nuntang S, Prasassarakich P. Adsorptive removal of thiophene and benzothiophene over zeolites from Mae Moh coal fly ash. *Fuel*. 2007; 87: 2347-2351.
69. Nikkolaj H, Brosrson M, Hen rik T. Activities of unsupported second transition series metal sulfides for hydrodesulfurization of sterically hindered 4,6 DMDBT and of unsubstituted DBT, *Catalysis Letters*. 2006; 65: 196-174.
70. Olmo CH, Almudena A, Victoria ES, Felix GO. Modeling the production of a *Rhodococcus erythropolis* IGTS8 biocatalyst for DBT biodesulfurization: Influence of media composition. *Enzyme and Microbial Technology*. 2005; 37: 157–166.
71. Paris-Marcano L. Process for recovering metals and for removing sulfur from materials containing them by means of an oxidative extraction. USA patent. 1992; 5: 087,350.

72. Park JG, Chang HK, Yi KB, Park JH, Han SS, Cho SH, Kim JN. Reactive adsorption of sulfur compounds in diesel on nickel supported on mesoporous silica. *Applied Catalysis B: Environmental*. 2008; 81: 244-250.
73. Parkinson G. Diesel Desulfurization Puts Refiners in a Quandery. *Chem. Eng.* 2000; 45-48.
74. Patrick ST, James RK, John WE. Desulfurization of fuel oil by oxidation and extraction, enhancement of extraction oil yield. *Ind. Eng. Chem. Res.* 1990; 29: 321-324.
75. Prasad VVDN, Kwang EJ, Chae HJ, Kim CU, Jeong SY. Oxidative desulfurization of 4,6-dimethyl dibenzothiophene and light cycle oil over supported molybdenum oxide catalysts. *Catalysis Communications*. 2008; 9: 1966-1969.
76. Qian W, Yoda Y, Hirai Y, Ishihara A, Kabe T. Hydrodesulfurization of DBT and hydrogenation of phenanthrene on alumina supported Pt and Pd catalysts. *Appl. Catal. A* 1991; 14: 81.
77. Reinhoudt HR, Troost R, Van Schalkwijk S, Van Langeveld AD, Sie ST, Van Veen JAR, Mouljin JA. Testing and characterization of Pt/ASA for deep HDS reactions. *Fuel Process Technol.* 1999; 61: 117.
78. Richard F, Biota T, Perot G. Reaction mechanism of 4, 6-methyldibenzothiophene desulfurization over sulfide NiMoP/Al<sub>2</sub>O<sub>3</sub>-zeolite catalysts. *Applied Catalysis A: General*. 2007; 320: 69-79.
79. Rodriguez-Castellon E, Jimenez-Lopez A, Eliche-Quesada D. Nickel and Cobalt promoted tungsten and molybdenum sulfide mesoporous catalysts for hydrodesulfurization. *Fuel*. 2007; 87: 1195-1206.
80. Sano Y, Sugaraha K, Choi K, Korai Y, Mochida I. Two-step adsorption process for deep desulfurization of diesel oil. *Fuel*. 2005; 84: 903-910.
81. Saterfield CN. *Heterogeneous catalysis in industrial practice*, 2<sup>nd</sup> Ed, McGraw-Hill: New York. 1993.
82. Selvavathi V., V. Chidambaram, A. Meenakshisundaram, B. Sairam, B. Sivasankar. Adsorptive desulfurization of diesel on activated carbon and nickel supported systems. *Catalysis Today* 141 (2009) 99-102.



83. Shafi R, Rafiq MH, Siddiqui, Graham J. Hutchings<sup>1</sup>, Derouane EG, Ivan V. Kozhevnikov. Heteropoly acid precursor to a catalyst for dibenzothiophene hydrodesulfurization. *Applied Catalysis A: General*. 2000; 204: 251–256.
84. Shavandi M, Majid S, Alireza Z, Khosro K. Biodesulfurization of dibenzothiophene by recombinant *Gordonia alkanivorans* RIPI90A. *Bioresource Technology*. 2009; 100: 475–479.
85. Shiraishi Y, Hara H, Hirai T, Komasaawa I. A deep desulfurization process for light oil by photosensitized oxidation using a triplet photosensitizer and hydrogen peroxide in an oil/water two-phase liquid-liquid extraction system. *Ind. Eng. Chem. Res.* 1999; 38: 1589-1595.
86. Shiraishi Y, Hara H, Hirai T, Komasaawa I. A novel desulfurization process for fuel oils based on the formation and subsequent precipitation of S-alkylsulfonium salts, *Ind. Eng. Chem. Res.* 2001; 40(22): 4919-4924.
87. Takahashi A, Yang FH, Yang RT. New sorbent for desulfurization by  $\pi$ -complexation: Thiophene/Benzene Adsorption. *Ind. Eng. Chem. Res.* 2002; 41: 2487.
88. Tam PS, Kittrell JR, Eldridge JW. Method of desulfurization and dearomatization of petroleum liquids by oxidation and solvent extraction. *Ind. Eng. Chem. Res.* 1990; 29: 321-324.
89. Tang K, Song L, Duan L, Li X, Gui J, Sun Z. Deep desulfurization by selective adsorption on a heteroatoms zeolite prepared by secondary synthesis. *Fuel processing technology*. 2008; 89: 1-6.
90. United Nations Environment Program.
91. Vargas-Villamil FD, Marroquín JO, Paz, Rodríguez E. A catalytic distillation process for light gas oil hydrodesulfurization. *Chemical Engineering and Processing*. 2004; 43: 1309–1316.
92. Venezia Am, Parola VL, DEganello G, Cauzzi D, Leonardi G, Predieri G. influence of the preparation method on the thiophene HDS activity of silica supported CoMo catalysts. *Appl. Catal. A*. 2002; 229: 261.

93. Wang H, Roel P. Hydrodesulfurization of dibenzothiophene, 4,6-dimethyldibenzothiophene, and their hydrogenated intermediates over Ni-MoS<sub>2</sub>/c-Al<sub>2</sub>O<sub>3</sub>. *Journal of Catalysis*. 2009; 264: 31–43.
94. Wang H, Song L, Jiang H, Xu J, Jin L, Zhang X, Sun Z. Effects of olefin on adsorptive desulfurization of gasoline over Ce(IV)Y zeolites. *Fuel Processing Technology*. 2009; 90: 835–838.
95. Wang Y, Latz J, Dahl R., Pasel J, Peters R. Liquid phase desulfurization of jet fuel by a combined pervaporation and adsorption process. *Fuel Processing Technology*. 2009; 90: 458–464.
96. Wangliang Li, Huang Tang, Qingfen Liu, Jianmin Xing, Qiang Li, DanWang, Maohua Yang, Xin Li, Huizhou Liu, Deep desulfurization of diesel by integrating adsorption and microbial method. *Biochemical Engineering Journal* 44 (2009) 297–301.
97. Weber Jr W.J., J.C. Morris, Kinetics of adsorption on carbon from solution, *J. Sanitary Engg. Div. ASCE* 89 (1963) 31-59.
98. Weitkamp J, M. Schwark, S. Ernst, Removal of thiophene impurities from benzene by selective adsorption in zeolite ZSM-5. *J. Chem. Soc. Chem. Commun.* (1991) 1133-1134.
99. Whitehurst DD, Isoda I, Mochida I. Present state of art and future challenges in hydrodesulfurization of polyaromatic sulfur compounds. *Advances in Catalysis*. 1998; 345-357.
100. Xiaoliang Ma, Anning Zhou, Chunshan Song, A novel method for oxidative desulfurization of liquid hydrocarbon fuels based on catalytic oxidation using molecular oxygen coupled with selective adsorption. *Catalysis Today* 123 (2007) 276–284.
101. Yang J, Yongqi H, Dishun Z, Shaozhao W, Peter CKL, Marison. Two-layer continuous-process design for the biodesulfurization of diesel oils under bacterial growth conditions. *Biochemical Engineering Journal*. 2007; 37: 212–218.
102. Yang L, Li J, Yuan X, Qi Y. one-step non-hydrodesulfurization of fuel oil: Catalysed oxidation adsorption desulfurization over HPWA-SBA-15. *Journal of molecular Catalysis A: Chemical*. 2007; 262: 114-118.
103. Yang RT, Maldonado A, Yang FH. Desulfurization of transportation fuels with zeolite under ambient conditions. *Science*. 2003; 301: 79.